Title

The role of folate receptor 1 in axon development

Author

Bischak, Kristina

Publication Date

2024

Peer reviewed|Thesis/dissertation

The role of folate receptor 1 in axon development

By

KRISTINA M. BISCHAK
DISSERTATION

Submitted in partial satisfaction of the requirements for the degree of

DOCTOR OF PHILOSOPHY

in

Molecular, Cellular, and Integrative Physiology

in the

OFFICE OF GRADUATE STUDIES

of the

UNIVERSITY OF CALIFORNIA

DAVIS

Approved:

Laura N. Borodinsky, Chair

Kassandra M. Ori-Mckenney

Sergi Simó

Committee in Charge

2024

ABSTRACT

During early nervous system development, neural stem cells exit the cell cycle and commit to the neuronal phenotype, after which begins the process of neurite outgrowth that gives rise to axons and dendrites. Axons are responsible for establishing and maintaining synaptic connections with target tissues during nervous system development, and are thus essential for the continued development and functionality of the central nervous system (CNS). Folate receptor 1 (Folr1), one of several folate uptake systems, is necessary for the formation of the neural tube, a process that occurs before neurons differentiate and adopt their neuronal morphology. Deficiency of Folr1 in developing vertebrate embryos leads to neural tube defects because of the failure of the neural tube to form and close. Whether Folr1 is important for later stages of spinal cord development is not yet known. Thus, the focus of my thesis is to investigate the role of Folr1 in axon development in the embryonic spinal cord. Here I show that Folr1 is expressed throughout the axons of embryonic spinal cord explants isolated from neural tube stage *X. laevis* embryos. Using a loss-of-function approach I show that knockdown of Folr1 in embryonic spinal cord explants results in axon retraction, as well as reduced βIII-tubulin enrichment in axons and altered filopodia production and actin dynamics in axonal growth cones. Moreover, I find that the elongation factor eEF1A2, a GTP-binding protein that non-canonically regulates F-actin dynamics, interacts and colocalizes with Folr1 in embryonic spinal cord neuron axons. Knockdown of Folr1 results in depletion of eEF1A2 and phospho(Ser^{358})-eEF1A2 in axons, and altered localization of eEF1A2 in growth cones. Taken together, these results indicate that Folr1 is important for axon outgrowth during spinal cord development and suggest that interaction of Folr1 with eEF1A2 facilitates proper function of cytoskeletal proteins important for growth cone dynamics.

ACKNOWLEDGEMENTS

I would like to acknowledge the many people who have helped me through graduate school and have made my thesis work possible:

A huge thank-you to Dr. Laura Borodinsky for being an amazing mentor and PI. I would not have been able to finish my graduate school journey without her incredible patience, kindness, and generosity. I am truly fortunate to have been able to have her as a mentor for my thesis work and I cannot thank her enough for the support she has given me, for the opportunity to work with and learn from her and everyone in her lab, and for all she has taught me about science. It is truly rare to find a PI so dedicated to helping their students in whatever way possible- troubleshooting experiments, talking through results and how best to present them, helping to perfect manuscripts and presentations, even helping with experiments if necessary- all with an incredible positive outlook and tenacity essential (I am convinced) to navigating the ups and downs of being a scientist.

Thank you to all of the wonderful scientists I was able to work alongside during my time in the Borodinsky lab: Olesya Visina, Olga Balashova, Andrew Hamilton, Raman Goyal, Alexios Panoutsopoulos, Sangwoo Shim, Kayla Sparks, Jacqueline Levin, and Andrea Navarrete Vargas. I am so grateful to have been able to work with and learn from such an amazing group of people, and truly appreciate everyone's support and companionship throughout my time in the lab.

I would especially like to thank Olga Balashova for her excellent doctoral and post-doctoral work in the Borodinsky lab exploring the role of Folr1 in neural tube closure in *Xenopus laevis*, upon which my project is largely based and would not exist without. A huge thank-you to Olga as well for all of her help with experimental procedures and troubleshooting; for teaching me techniques essential for my project; for sharing her constructs and reagents; for her patience in answering my many questions and engaging in late-night chats about experimental details; and for generally being a fantastic person and scientist.

I would also like to thank Dr. Julie Bossuyt and Dr. Eleanora Grandi for their support throughout my time in the MCIP program, and my Dissertation Committee members, Dr. Sergi Simó and Dr. Kassandra Ori-Mckenney, for their time, consideration, and helpful comments regarding my work and manuscript.

Finally, I would like to thank my family for their love and support, without which I would not have been able to make it to or through graduate school.

TABLE OF CONTENTS

INTRODUCTION

Folate

Folate belongs to the B9 family of vitamins and functions primarily as a mediator of one-carbon metabolic reactions such as those involved in nucleotide and amino acid biosynthesis, DNA replication and repair, and DNA methylation (Choi & Mason, 2002; Stover, 2004). It cannot be synthesized *de novo* in animals and thus must be obtained through dietary sources in the form of dihydrofolate, tetrahydrofolate, and 5-methyltetrahydrofolate, or as synthetic folic acid in fortified foods (Eitenmiller et al., 2007; Lewis et al., 1999).

Folate deficiency correlates with an increased incidence of neural tube defects (CDC, 1992; MRC Vitamin Study Research Group, 1991; Smithells et al., 1976). These birth defects are multifactorial and occur by the fourth week of pregnancy due to failure of the neural plate to fold and the neural tube to form and close during these early stages of nervous system development (Wallingford et al., 2013). Periconceptional folate supplementation has been proven to diminish the prevalence of neural tube defects (Berry et al., 1999; Blom et al., 2006; MRC Vitamin Study Research Group, 1991).

The role of folate in later stages of neural development remains unexplored. Intriguingly, administration of folate was used as an epilepsy model several decades ago but without a clear mechanistic understanding of how it altered synaptic activity in varied preparations (Baxter et al., 1973; Hill & Miller, 1974; R. G. Spector, 1972). There is also a body of work showing that folate deficiency contributes to neurodegeneration by dysregulating oxidative stress (Mattson & Shea, 2003; Miranda-Morales et al., 2017). Particularly relevant to my investigation, folic acid supplementation promotes axon regeneration of peripheral nerves (Harma et al., 2015; Kang et al., 2019), and in a sciatic nerve injury rat model it was found to do so through a folate receptor 1-dependent mechanism (Iskandar et al., 2004, 2010).

Folate receptor 1

Folates are hydrophilic and cannot be synthesized *de novo* in mammals; therefore, facilitated transport of folates into cells is required for its participation in cell metabolism (Zhao et al., 2009). There are three main folate transport systems in mammals: reduced folate carrier (RFC), proton-coupled folate transporter (PCFT), and folate receptors. RFC, also known as SLC19A1, is a member of the SLC family of transporters and is ubiquitously expressed in human tissues and malignant tumor cell lines (Whetstine et al., 2002) and widely in murine tissues (Wang et al., 2001). RFC functions optimally at neutral pH and has high affinity (Km ~ 3-7 μM) for reduced forms of folate (5-methyltetrahydrofolate and 5-formyltetrahydrofolate) but low affinity for folic acid (Ki ~150-200 μM), and due to its ubiquitous expression in tissues, is expected to function generally to maintain folate homeostasis (Matherly & Goldman, 2003; Zhao et al., 2009). PCFT, also known as SLC46A1, is expressed in a number of tissues such as placenta, liver, and the apical brush border of kidneys and intestines in rodents and humans (A. Qiu et al., 2006, 2007). Due to its increased affinity (Km~ 0.5-1 μM) for reduced (5-methyltetrahydrofolate and 5-formyltetrahydrofolate) and oxidized (folic acid) forms of folate at low pH, it is particularly important for the uptake of dietary folate in the duodenum and upper jejunum of the small intestine (A. Qiu et al., 2006; Schron et al., 1985; Zhao & Goldman, 2007). Indeed, mutations in PCFT but not RFC result in hereditary folate malabsorption in human patients (A. Qiu et al., 2006), thus demonstrating the importance of this transporter for tissue and serum folate levels in mammals. Folate receptors include Folr1, also known as FRα, Folr2/FRβ, and Folr3/FRγ. Folr1 and Folr2 are glycosylphosphatidylinositol (GPI)-anchored proteins that are highly homologous and have high affinity for folic acid (Kd 1-10 nM) but differ in their expression patterns and binding specificities for folates (Ross et al., 1994; Zhao et al., 2009), while Folr3 is a secreted form of the protein that lacks a GPI anchor and is only expressed in hematopoietic tissues (Matherly & Goldman, 2003; Shen et al., 1995). Much of the research performed to date regarding folate receptors during early development has focused on Folr1, which is the primary focus of my investigation.

Folr1 facilitates folate uptake via endocytosis (Antony, 1996; Sabharanjak & Mayor, 2004) and is primarily found in the placenta, the choroid plexus, and the brush border membrane of the kidney (Antony, 1992; Elwood, 1989; Holm et al., 1991; Prasad et al., 1994; Selhub & Franklin, 1984; R. Spector, 1977), as well as the neural folds and neural tube of mouse (Piedrahita et al., 1999; Saitsu et al., 2003) and neural plate of *Xenopus laevis* (Balashova et al., 2017) embryos. Folr1 is important for the uptake of folate, particularly in low-folate environments (Matsue et al., 1992). Knockout or knockdown of Folr1 results in neural tube defects in mice (Piedrahita et al., 1999) and *Xenopus laevis* embryos (Balashova et al., 2017). In addition, mutations in human FOLR1 that prevent its localization to the plasma membrane have been linked to clinical cases of cerebral folate transport deficiency, a condition that results in severe neurodevelopmental delays, epilepsy, and ataxia (Grapp et al., 2012). In our lab, we have found that Folr1 is necessary for neural tube formation in *X. laevis* embryos, and that Folr1 interacts with cell adherens junction molecules C-cadherin and β-catenin to facilitate apical constriction of neural plate cells during neural plate folding (Balashova et al., 2017). The role of Folr1 in later stages of neural development, after the neural tube is formed, and specifically regarding the acquisition of neuronal morphology, has not been investigated before.

Axon morphogenesis

As soon as neural stem cells exit the cell cycle and commit to the neuronal phenotype, neuron-specific cytoskeletal proteins are expressed to enable acquisition of neuronal morphology essential for establishing neural circuits and nervous system function. Neurite outgrowth that gives rise to axons and dendrites becomes apparent early on during the process of neuronal differentiation. Axons extend from the neuronal soma outward, reaching varied lengths depending on the location of their target cells with the goal of forming synapses for the relay of information from the nervous system to target tissues (Koenig, 2009; Letourneau, 2009; Pacheco & Gallo, 2016). Crucial to the structural integrity of axons is the cytoskeletal network, made up of microtubules, microfilaments, and intermediate filaments (**Fig. 1**). Microtubules are

rod-like structures consisting of α- and β-tubulin monomers arranged in a helical rod shape. Microtubules are arranged in the axon shaft as rods of varying length (**Fig. 1**) and oriented with the plus-end pointing away from the soma in order to establish polarity (Dent & Gertler, 2003; Falnikar & Baas, 2009). There are numerous isotypes of both α- and β-tubulin that, although not well understood, are thought to contribute to the diverse developmental stage-, cell type-, and organism-specific differences in tubulin behavior and function (Joshi & Cleveland, 1989; Nsamba & Gupta, 2022; Tischfield & Engle, 2010). An important property of microtubules is their 'dynamic instability', referring to the continual polymerization and depolymerization process that takes place in the axon, and especially in more dynamic regions such as the growth cone, the distal tip of the growing axon (Dent et al., 2011; Dent & Gertler, 2003; Falnikar & Baas, 2009). Post-translational modifications (PTMs) of α- and β-tubulin, such as acetylation, tyrosination, glutamylation, and glycylation, can affect interaction of certain proteins with microtubules as well as overall polymerization and depolymerization rates (Baas & Black, 1990; Gadadhar et al., 2017; Sanyal et al., 2023). In addition to PTMs, various microtubule associated proteins (tau, MAP1a), plus-end binding proteins (EB1, CLIPs, CLASPs), and severing proteins (katanin, spastin) also regulate microtubule dynamics, generally in favor of polymerization and stabilization of microtubules in order to promote growth and stability of the axon (Falnikar & Baas, 2009; Matus, 1990; Tirnauer et al., 2002). In addition to providing structural support for the axon shaft, microtubules also function as tracks upon which cellular transport of organelles, vesicles, and other materials takes place, a function that is indispensable for the growing axon (Dent et al., 2011).

Equally important for axon structural integrity and function are microfilaments, composed of filamentous (F)-actin polymers. In the axon shaft, actin filaments form consecutive rings beneath the plasma membrane (**Fig. 1**) that, along with spectrin, create a structural scaffold (D'Este et al., 2015; Leterrier et al., 2015; K. Xu et al., 2013). F-actin is particularly important for proper structure and functioning of the growth cone. Growth cone structure is often divided into three regions: the peripheral domain, central domain, and transition zone (Bridgman & Dailey, 1989; Lowery & Vactor, 2009). Within the peripheral domain,

lamellipodia (sheet-like) and filopodia (filament-like) structures composed of F-actin (**Fig. 1**) constantly extend and retract to explore the environment and advance the axon along substrate and extracellular structures (Bridgman & Dailey, 1989; Dent & Gertler, 2003). This dynamic actin activity, often referred to as treadmilling, is regulated by an ever-growing list of molecules known as actin-binding proteins (ABPs), which perform a variety of functions such as end-capping of actin monomers and severing, cross-linking, and branching of actin polymers (Dent & Gertler, 2003; Pollard, 2016). A few of the more widely-studied ABPs include cofilin, which binds to actin monomers (globular or G-actin) to inhibit polymerization of new filaments, as well as sever existing filaments; profilin, which has the opposite effect on ATP binding and polymerization rate (Bamburg, 1999; Nishida, 1985); and gelsolin, a large calcium-activated protein which severs actin polymers and caps the barbed end of filaments to prevent polymerization (Janmey & Stossel, 1987; Pollard, 2016).

Crosstalk between actin and tubulin is also important for axon outgrowth. Within the peripheral domain and transition zone of the growth cone, filopodia composed of F-actin filaments anchor the growth cone to the substrate or extracellular structure, and web-like lamellipodia structures extend along this scaffold followed closely by dynamic microtubules rich in tyrosinated α-tubulin (Letourneau, 2009; Pacheco & Gallo, 2016). Although relatively few microtubules branch out into the growth cone beyond the central domain, the extension of microtubules into these regions allows for greater structural integrity and for communication with the rest of the axon, and facilitates polymerization of microtubules for axon growth (Dent & Gertler, 2003; Letourneau, 2009). This continuous ebb and flow of actin and tubulin within this dynamic region allows for the steady growth of the axon. Additionally, the concerted efforts of both microfilaments and microtubules within the growth cone facilitates growth cone turning in response to chemoattractant or -repulsive factors and other environmental guidance cues (Tessier-Lavigne & Goodman, 1996). In this way, a delicate and constantly-shifting balance between extension and retraction, growth and disassembly, within both the microfilament and microtubule populations, drives axon growth and pathfinding.

Intermediate filaments (IF), so named for their size (8-10 nm) in comparison to microfilaments (6-8 nm) and microtubules (24-26 nm), are another major structural component of axons (Liem & Messing, 2009). The IF family of proteins is a diverse group consisting of nearly 50 different proteins organized into six groups (type I-VI), the expression of which varies widely based on cell type and function (Cooper, 2000). Neurons of the central nervous system mainly express type IV IF proteins, which includes α-internexin and the neurofilament triplet proteins (NFTPs): neurofilament light (NF-L), neurofilament medium (NF-M), and neurofilament heavy (NF-H) (Barry et al., 2007; Liem & Messing, 2009). Nestin and vimentin are also transiently expressed in neurons, but only in neural progenitor cells prior to differentiation (Fuchs & Weber, 1994; Lee & Cleveland, 1996). Generally, each neurofilament is assembled from a combination of NF-L, NF-M, NF-H, and α-internexin monomers which form coiled-coil heterodimers that connect laterally to form non-polar tetramers; eight tetramers then come together to form a unit length filament (ULF) of 60 nm, and many ULFs assemble end-to-end to form a neurofilament (Yuan et al., 2017). Neurofilaments also have "side arms" formed from the C-terminal tails of NF-H and NF-M monomers that extend outwards from the filament that are thought to form a bridge between filaments to improve structural integrity of axons (Barry et al., 2007; Lee & Cleveland, 1996). Neurofilaments are primarily expressed in mature axons, and are especially present in myelinated motor neuron axons where they can outnumber microtubules 5-10 fold (Barry et al., 2007; Lee & Cleveland, 1996). Neurofilaments form a scaffold within the cytoplasm that provides structural support (Fuchs & Cleveland, 1998), helps to regulate the diameter of myelinated axons (Fuchs & Weber, 1994; Lee & Cleveland, 1996), and facilitates the transport and docking of synaptic vesicles, endosomes, and organelles such as the endoplasmic reticulum (ER) and mitochondria (Rao et al., 2011; Wagner et al., 2003; Yuan et al., 2017). In addition, various linker proteins connect neurofilaments to microtubules and microfilaments in order to form a cohesive cytoskeletal structure and network essential to the function and structural integrity of axons (Fuchs & Cleveland, 1998; Hisanaga & Hirokawa, 1990).

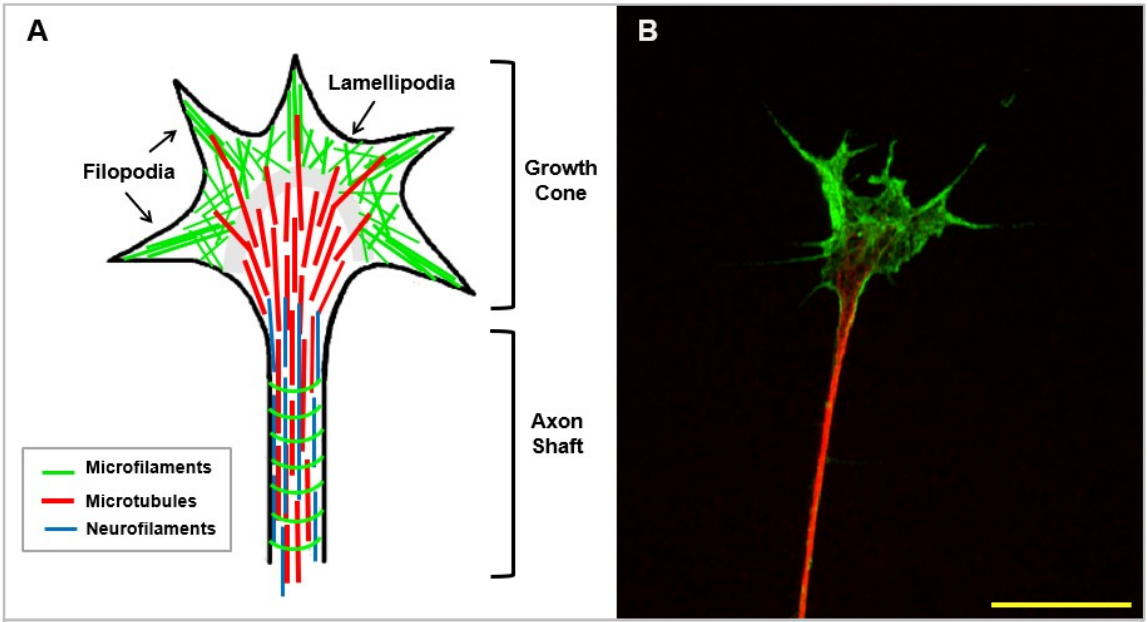

Figure 1. Cytoskeletal organization in axons. A) Stylized depiction of the cytoskeletal structure consisting of F-actin microfilaments (green), microtubules (red), and neurofilaments (blue) throughout the axon shaft and growth cone. The gray region delineates the transition zone, located between the F-actin enriched peripheral domain and the tubulin enriched central domain. **B)** Representative immunofluorescence image of an embryonic spinal cord neuron axon grown *in vitro* for 16 h and labeled for F-actin (green, Phalloidin-AlexaFluor 488) and βIII-tubulin (red, anti-βIII-tubulin immunostaining).

Elongation factor 1 alpha

The eukaryotic elongation factor 1 alpha (eEF1A), also known as translation elongation factor 1 alpha, is a GTP-binding protein that facilitates the transfer of aminoacyl t-RNAs during the elongation stage of protein synthesis (Negrutskii & El'skaya, 1998). It functions as a complex with the catalytically active beta subunit (eEF1B), known previously as the heavy subunit (EF1-H), which is made up of alpha (eEF1Bα), delta (eEF1Bδ), and gamma (eEF1Bγ) subunits and facilitates the exchange of GTP and GDP (Janssen et al., 1994; Negrutskii & El'skaya, 1998). The alpha subunit is present in two isoforms, eEF1A1 and eEF1A2, which are 92% identical but differ in their spatiotemporal expression (S. Lee et al., 1992, 1993). Whereas eEF1A1 is nearly ubiquitously expressed, eEF1A2 is primarily found in neural, heart, and muscle tissue, and its expression in these tissues occurs later in development, around 14 days after birth in mice and rats (S. Lee et al., 1992, 1993) and beyond neural tube formation stages in *X. laevis* (Abdallah et

al., 1991; Djé et al., 1990; Krieg et al., 1989), concomitant with a decline in eEF1A1 expression. This switch in expression is crucial for the development of these tissues during cell differentiation (S. Lee et al., 1995).

In addition to its role in protein elongation, eEF1A2 is involved in numerous other cellular processes. Mutations in the eEF1A2 gene result in neurodevelopmental and neuromuscular delays and disorders in both mice (Davies et al., 2020; Shultz et al., 1982) and humans (De Rinaldis et al., 2020; Lam et al., 2016; Nakajima et al., 2015). In mice, a mutation in the eEF1A2 gene that deletes the promoter and first exon, resulting in lack of expression, was found to be responsible for the "wasted"/*wst* phenotype, which results in loss of muscle tone, tremors, and ataxia by day 21 after birth and death by four weeks (Chambers et al., 1998; Shultz et al., 1982). Vacuolar degeneration of the anterior horn cells of the spinal cord and retraction of axons from motor nerve end plates, as well as degeneration of Purkinje cells, demyelination of the cerebellar cortex, and abnormalities in the immune and lymphoid systems were also observed in homozygous *wst*/*wst* mice (Abbott et al., 2009; Shultz et al., 1982; Woloschak et al., 1987). Similarly, *de novo* missense mutations in the eEF1A2 gene have been identified in human patients presenting with epilepsy, neurodevelopmental delays, and neuromuscular disorders (De Rinaldis et al., 2020; Lam et al., 2016; Nakajima et al., 2015).

Gain of eEF1A2 function has been identified as oncogenic. Upregulation or overexpression of eEF1A2 has been linked to increased tumorigenesis and metastatic behaviors in ovarian (Anand et al., 2002), breast (Amiri et al., 2007; Tomlinson et al., 2005), liver (Qui et al., 2016), and lung tumors and cell lines (Lam et al., 2006; Zhu et al., 2007), and poor prognosis in gastric (Yang et al., 2015) and prostate (Worst et al., 2017) cancers. Possibly related to its proposed role as an oncogene, eEF1A2 has also been found to inhibit apoptosis (Chang & Wang, 2007; Ruest et al., 2002) and to activate the PI3K/Akt/NF-κB pathway (Amiri et al., 2007; F.-N. Qiu et al., 2016).

Other functions of eEF1A include binding to and interacting with F-actin and F-actin bundles in yeast (Gross & Kinzy, 2005; Munshi et al., 2001) and in *in vitro* polymerization and binding assay

experiments (Murray et al., 1996). eEF1A2 binds to β-actin mRNA and facilitates bundling of F-actin in dendritic spines of mouse embryonic hippocampal cultures (Mendoza et al., 2021). eEF1A also interacts with microtubules (Shiina et al., 1994) and with phosphatidylinositol-4-kinase III β (Jeganathan et al., 2008). The purpose of these additional roles of eEF1A1 and 2 is still unclear; however, in the case of eEF1A2 interacting with actin and other cytoskeletal elements, it has been proposed that this may provide a mechanism through which cytoskeletal protein levels can be regulated in specific cellular compartments during highly dynamic processes involving cytoskeletal rearrangement (Mendoza et al., 2021; Murray et al., 1996). Interestingly, phosphorylation at several actin-related phosphorylation sites not found on eEF1A1, including Ser^{358}, inhibits the protein synthesis function of eEF1A2, reduces its affinity for F-actin, and increases actin dynamics in dendritic spines from mouse hippocampal neuron cultures (Mendoza et al., 2021).

Neural development in Xenopus laevis embryos

The neural tissue arises from the ectoderm during a process known as neural induction (Lallier & DeSimone, 2000). Soon after, neural cells organize into the neural plate, a flat structure consisting of a double layer of cells in *Xenopus laevis* embryos (Davidson & Keller, 1999). The neural plate then folds inwards, a morphological change facilitated by apical constriction of the outer layer of cells, in order to form the neural tube during neurulation (Balashova et al., 2017; Catala, 2005). Once the neural tube closes, neurons begin to differentiate, and the posterior section of the neural tube becomes the embryonic spinal cord while the anterior develops into the embryonic brain (Betts et al., 2022; Huxley & De Beer, 1934). By 22-24 hours post fertilization (hpf; when grown at 23°C (Nieuwkoop & Faber, 1994)), neurons in the embryonic spinal cord start to grow axons in order to reach their synaptic targets (Gomez & Spitzer, 1999; Taylor & Roberts, 1983).

X. laevis has been used extensively as a model organism to study neurodevelopment (Borodinsky, 2017; Gomez & Spitzer, 1999; Taylor & Roberts, 1983). *X. laevis* embryos can be procured easily through *in vitro* fertilization with excised testis and harvested oocytes (Sive et al., 2010). Following fertilization, development of *X. laevis* embryos progresses quickly, is easily observable with the naked eye or under low magnification scopes, and the developmental rate can be adjusted by changing the temperature of the bath solution to meet experimental needs (Nieuwkoop & Faber, 1994; Sive et al., 2010). In particular, the process of neurulation can be observed externally and is thus easy to track and image (Borodinsky, 2017; Wallingford, 2010). Cultures of *X. laevis* embryonic spinal cord tissue, such as dissociated embryonic spinal cord neurons or embryonic spinal cord explants, can be grown at room temperature (23°C) in modified saline solution and thus can also be live imaged at room temperature (Erdogan et al., 2021). In addition, manipulation of gene or protein expression is relatively simple through the injection of morpholinos, mRNA, or DNA during early development that allows for global or tissue-specific manipulation (Borodinsky, 2017; Sive et al., 2010; Slater et al., 2017).

X. laevis is also an excellent model for examining axon growth and morphology. As mentioned previously, cultured explants or dissociated neurons derived from the embryonic spinal cord can be grown at room temperature in modified saline solution and can be used for many experimental applications (**Fig. 2**). In addition, *X. laevis* growth cones are large (10-30 μm) in comparison to other vertebrate growth cones (Lowery et al., 2012; Slater et al., 2017) and are thus ideal for use in experiments examining axon growth and pathfinding, growth cone dynamics, and cytoskeletal protein organization and dynamics within growth cones. Indeed, *X. laevis* embryos and embryonic spinal cord neurons have been used in studies examining calcium activity during axon outgrowth, both *in vivo* (Gomez & Spitzer, 1999) and *in vitro* (Gomez et al., 2001); to track axon growth and pathfinding in the developing *X. laevis* spinal cord (Roberts & Clarke, 1982; Taylor & Roberts, 1983); and to track axonal growth cone dynamics (Song et al., 1997; X. Xu et al., 2005; Zheng et al., 1996). *X. laevis* spinal cord neurons have also been used by numerous labs to examine cytoskeletal organization and protein expression in growth cones (Lowery et al., 2013; Lucaj et al., 2015;

Marx et al., 2013). Experiments involving the optical nerves of *X. laevis* embryos to examine axon growth and regeneration (McFarlane & Lom, 2012; Ruchhoeft et al., 1999; Santos et al., 2020; Shirkey et al., 2012) have also been performed extensively, further highlighting the versatility of this model system.

In my study, I utilize *X. laevis* embryonic spinal cord explants isolated from neural tube stage (stage 22-23; 24-24.75 hpf) embryos to examine the necessity of Folr1 for axon growth in the developing spinal cord. Using a knockdown approach, I examine the effect of reduced Folr1 expression on several aspects of axon growth and development through experiments involving live imaging of axon growth, analysis of axonal protein expression and localization through immunofluorescence confocal imaging and Western Blot assays, and live imaging of actin dynamics in axonal growth cones (**Fig. 2**).

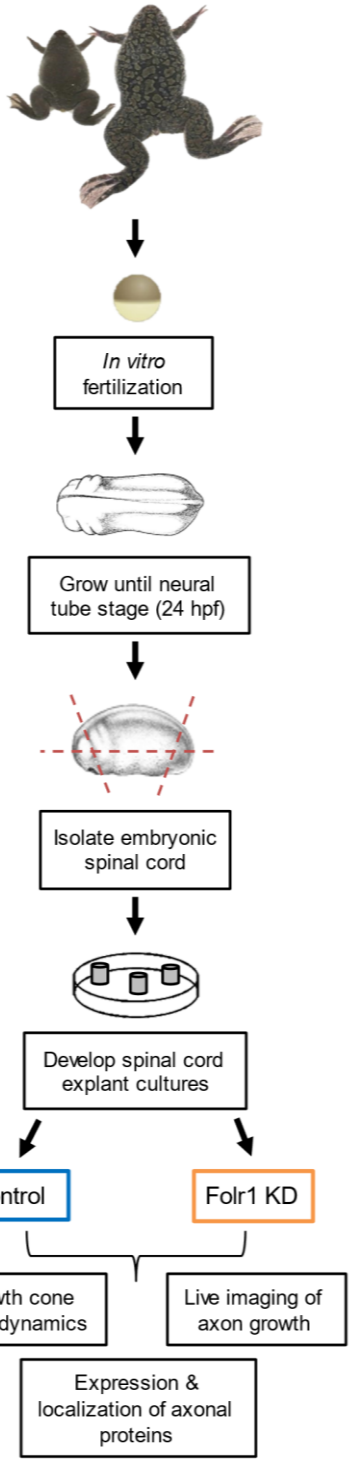

Figure 2. Research strategy for the study of Folr1-dependent *Xenopus laevis* spinal cord neuron axon growth. Schematic outlining the use of *X. laevis* embryonic spinal cord explants in experiments examining protein expression and localization in axons, axon growth *in vitro*, and growth cone actin dynamics in Folr1-knockdown (Folr1 KD) and control samples. Embryo staging images courtesy of Xenbase.org (Fisher et al., 2023) and the Normal table of *Xenopus laevis* development (Nieukwoop & Faber, 1994).

EXPERIMENTAL PROCEDURES

In vitro fertilization of Xenopus laevis oocytes

Mature oocytes were collected in a cell culture dish containing 1X Mark's Modified Ringer (MMR) solution (100 mM NaCl, 2 mM KCl, 1 mM $MgSO_4$, 5 mM Hepes, 50 mM EDTA and 2 mM $CaCl_2$, pH 7.8) from a female frog injected with human chorionic gonadotropin hormone 16 h before collection. Eggs were washed and a piece of testes was then minced in the dish and rapidly flushed with deionized water to achieve a 10% MMR solution; this is considered time 0 of fertilization. Fertilized oocytes were kept in 10% MMR (10 mM NaCl, 0.2 mM KCl, 0.1 mM $MgSO_4$, 0.5 mM Hepes, 5 mM EDTA and 0.2 mM $CaCl_2$, pH 7.8).

Microinjection of 2-4 cell stage embryos

Mature oocytes were fertilized as described above and grown at 23°C for 1 h. Embryos were then de-jellied by incubating in 2% cysteine solution (Sigma Aldrich, Cat# 168149; dissolved in 1x MMR, pH 8) for 2 min, followed by 5-6 washes with 10% MMR. Dejellied embryos were allowed to develop to 2-4 cell stage (1.5-2 h post fertilization (hpf); Nieuwkoop & Faber, 1994) at 23°C, then transferred to a 60 mm culture dish containing 6% Ficoll (Ficoll PM 400; Sigma-Aldrich, Cat# F4375) in 10% MMR. Microinjections were performed with pulled borosilicate glass capillaries (Warner Instruments, Cat# 64-0799), and each embryo was bilaterally injected to achieve a total mRNA concentration of 150-250 pg/embryo for LifeAct-eGFP mRNA (pCS2+Lifeact-eGFP plasmid gifted by Rusty Lansford; Addgene, Plasmid #128428). Injected embryos were kept in 6% Ficoll for a minimum of 1 h before being transferred to 35 mm culture dishes containing 10% MMR for the remaining growth period.

Embryonic spinal cord explant cultures

Xenopus laevis embryos were grown in 10% MMR at 23°C until stage 22-23 (24-24.75 hpf; Nieuwkoop & Faber, 1994), when spinal cord neurons are differentiating and neurites outgrowing (Taylor & Roberts, 1983). Embryos were then placed in a saline solution (4.7 mM Tris, 116 mM NaCl, 0.67 mM KCl, 1.3 mM $MgSO_4$, 2 mM $CaCl_2$, pH 7.8) and the posterior neural tube along with the notochord and somites were transferred to a dish containing freshly prepared 1 mg/ml collagenase B (Roche, Cat# 11088815001) and incubated at room temperature for 10 min. The tissues were then transferred to a fresh dish of culture medium where the remaining yolk, somites, notochord, and non-neural ectoderm were removed. The isolated neural tube was segmented into evenly sized sections with a tungsten wire tool and transferred to glass bottom culture dishes (Lab-Tek II Chambered Coverglass, 4-well, #1.5 Borosilicate coverslip; ThermoFisher, Cat# 155382), coated with Matrigel and containing saline culture medium (4.7 mM Tris, 116 mM NaCl, 0.67 mM KCl, 1.3 mM $MgSO_4$, 2 mM $CaCl_2$, 0.125 mg/mL gentamicin (Sigma-Aldrich, Cat# G1397), 25 units/mL penicillin, 25 µg/mL streptomycin (penicillin-streptomycin solution; Sigma-Aldrich, Cat# P4333), pH 7.8; filtered through a 0.2 µM-pore size syringe filter), using a glass Pasteur pipette. To coat the 4-well glass bottom culture dishes, Matrigel (growth factor reduced, phenol-red free; Corning, Cat# 356231) was diluted 1:100 in cold saline solution and 1 mL of diluted Matrigel solution was added to each well of the glass bottom culture dish and incubated for 1 h at 23°C. The remaining solution in the wells was removed and replaced with freshly made saline culture medium prior to addition of embryonic spinal cord explants or dissociated cells.

Dissociated spinal cord neuron cultures

The posterior neural tube, isolated as described above, was transferred to a culture dish containing dissociation saline medium (4.62 mM Tris, 0.41 mM EDTA, 116 mM NaCl, 0.67 mM KCl, pH 7.8) for 20-30 min and plated with a pulled glass Pasteur pipette in glass bottom culture dishes coated with Matrigel as described above and containing saline culture medium.

Folr1 knockdown in embryonic spinal cord explants

For knockdown of Folr1 in cultured embryonic spinal cord explants, a splicing-blocking vivo-morpholino (Folr1 v-MO) was custom ordered from Gene Tools (Gene Tools LLC., Philomath OR). The Folr1 v-MO sequence is complimentary to a 25-base pair region between the second exon and second intron of the *X. laevis folr1* mRNA, designed to prevent excision of the second intron (sequence: 5'-ATCACCCCCTTCCAATTACCTTCTG- 3'). The standard control v-MO (Control v-MO) developed by Gene Tools (sequence: 5'- CCTCTTACCTCAGTTACAATTTATA- 3') was used as a control. Stock solutions of v-MOs were made by reconstituting lyophilized powder to 0.5 mM with PCR grade nuclease-free water and were diluted to 0.1-0.5 μM working concentration. Folr1 and Control v-MOs were added to saline culture medium 0.5-4 h after plating of embryonic spinal cord explants for a duration of 5-18 h, depending on the experiment as detailed below.

Western Blot Assays

Embryonic spinal cords were isolated from stage 22-23 embryos (24-24.75 hpf), sectioned into explants and plated on Matrigel-coated glass bottom culture dishes in saline culture medium, as detailed above. Control or Folr1 v-MO was added to saline culture medium 1 h after plating at 0.2 μM for 18 h at 23°C. Embryonic spinal cord explants from 5 embryos were used per Control and Folr1 v-MO-treated lysate samples. To prepare lysates, cell lysis solution (0.5% SDS, 3 mM EDTA, 3 mM EGTA, protease inhibitor cocktail 1:100 ("Halt" Protease inhibitor cocktail, EDTA-free; Thermo Scientific, Cat# 87785), phosphatase inhibitor cocktail, 1:100 (Sigma-Aldrich, Cat# P5726)) was added to cell culture wells and incubated for 10 min with vigorous shaking. Lysates were collected and spun down at 26,000 RPM at 4°C for 10 min. The supernatant was then collected and 25% (v/v) protein loading buffer (250 mM Tris-HCl, pH 6.8; 8% SDS; 40% (w/v) glycerol; 0.01% Bromophenol Blue (Sigma-Aldrich, Cat# 114391)) and 1.25% (v/v) beta-

mercaptoethanol (Sigma, Cat# M6250) were added before boiling at 100°C for 5 min in a heating block. Samples were then run on 8-16% gradient SDS-PAGE gels (Bio-Rad, Cat# 4561105) at 95 V and transferred to a PVDF membrane. Transfer membranes were incubated in 5% milk (nonfat dry milk; Signature Select) in Tris-buffered saline containing 0.1% Tween 20 (TBST; 20 mM Tris, 150 mM NaCl, pH 7.6) and probed with anti-Folr1 antibody (GenScript; custom order anti-Folr1 polyclonal rabbit antibody designed against peptide sequence KHQKVDPGPEDDLHC, corresponding to a 15-amino acid C-terminus region of the *X. laevis* Folr1 protein), 1:500, followed by donkey anti-rabbit HRP secondary (Jackson Immunoresearch, Cat #711-035-152), 1:1,000. Membranes were stripped and re-probed with anti-Gapdh antibody (Sicgen, Cat# AB0049-20), 1:1,000, followed by anti-goat HRP secondary (RnD, Cat# HAF109), 1:10,000. For imaging, blots were incubated with Pierce ECL 2 Western Blotting substrate (ThermoFisher, Cat #80196) and imaged with the ChemiDoc MP Imaging System (Bio-Rad, Hercules CA). Images were analyzed with Image Lab software (Bio-Rad, Hercules CA).

Immunostaining of spinal cord explant and dissociated neuronal cultures

Embryonic spinal cord explants were isolated from stage 23 *Xenopus laevis* embryos and transferred to Matrigel-coated glass bottom culture dishes containing saline culture medium, as described above. Explants were grown at 23°C for 6-18 h, then fixed for 10 min with 4% paraformaldehyde (Sigma Aldrich; Cat# 158127) in phosphate buffered saline (PBS; 137 mM NaCl, 2.7 mM KCl, 4.3 mM Na_2HPO_4). Fixed samples were then incubated in permeabilizing buffer (0.5% Tween 20 (Sigma, Cat# T2700) in PBS; sterile) followed by blocking buffer (2% bovine serum albumin (Sigma, Cat# A3059) and 0.1% Tween 20 in PBS; sterile), both for 30 min at 23°C. Primary antibodies targeting proteins of interest were then diluted into blocking buffer, added to appropriate wells, and incubated overnight at 4°C. After washing out cultures, fluorescently-conjugated secondary antibodies were also diluted in blocking buffer and incubated with samples at 23°C for 2 h. Primary antibodies used: anti-Folr1, 1:2,000 (GenScript, custom); anti-Folr1,

1:1,000 (Boster Bio; custom order polyclonal rabbit antibody designed against the whole *X. laevis* Folr1 protein); anti-eEF1A2, 1:3,000 (Proteintech, Cat# 66806-1-IG); anti-phospho eEF1A2 (Ser^{358}), 1:700 (Invitrogen, Cat# PA5-35404); anti-βIII-tubulin, 1:900 (Millipore, Cat# AB9354); anti-acetylated α-tubulin, 1:2,000 (Santa Cruz, Cat# SC-23950); anti-tyrosinated α-tubulin, 1:1,000 (Millipore, Cat# MAB1864-I). Alexa Fluor 488-Phalloidin (Life Technologies, Cat# A12379) was diluted 1:50 in blocking buffer and incubated for 45 min at 23°C to label fibrillar actin. Samples were imaged on an inverted Nikon Eclipse T*i*2 C2 confocal microscope with 10x air and 20x, 60x, and 100x oil immersion objectives. Images were analyzed with NIS-Elements software (Nikon Instruments Inc., Melville NY).

Live imaging of actin dynamics in embryonic spinal cord neuron growth cones

Embryos were dejellied in 2% cysteine solution and injected with 150 pg LifeAct-eGFP mRNA (Addgene, Plasmid #128428) per embryo, as described above. Injected embryos were grown to stage 23 (24.75 hpf) and screened for expression of the construct with a Nikon AZ100 Stereoscope (Nikon Instruments Inc., Melville NY) prior to experimental use. Embryonic spinal cord explants were isolated from LifeAct-eGFP expressing embryos and plated in Matrigel-coated glass bottom culture dishes containing saline culture medium as described above. Folr1 v-MO or Control v-MO at 0.2 μM was added to saline culture medium 30 min after plating, and explants were grown at 23°C for 5 h. Time-lapse recordings of axons were taken with a Nikon T*i*2 Eclipse C2 confocal microscope using the 60x oil immersion objective. Images were taken every 20 s for 15 min. Actin-disrupting drugs Cytochalasin-D (Cyto-D; Tocris, Cat# 1233) and Jasplakinolide (Jasp; Santa Cruz, Cat# 102396-24-7) were dissolved to 0.5 mM in 100% DMSO (Fisher Scientific, Cat# BP231) and added to saline culture medium to final concentrations of 0.1 μM (Cyto-D) or 0.5 μM (Jasp) directly prior to the start of time-lapse recordings.

Co-Immunoprecipitation Assays

Neural tube, notochord, somites, and non-neural ectoderm were isolated together from stage 23 (24.75 hpf) embryos (10 per lysate) and processed in lysis buffer containing either 1% CHAPS (ThermoFisher, Cat# BP571-1) or 0.5% Sarcosyl (N-lauroylsarcosine sodium salt; Sigma-Aldrich, Cat# L5777) and 1% Triton X-100 (Sigma, Cat# X100). Lysates were then incubated with Agarose G beads (Roche, Cat# 10060957) crosslinked to 20 µg Folr1 antibody (GenScript, custom) or normal rabbit IgG (control) (Cell Signaling, Cat# 2729S) for 16 h at 4°C. Samples were spun down and supernatant was collected (Control and Folr1 flow-through lysate). Co-immunoprecipitated (IP) proteins were then dissociated from beads by boiling at 80°C for 10 min in 10 mM dithiothreitol (DTT) (ThermoFisher, Cat# 50591949). IP samples and lysates were then assessed via Western blot assays for proteins of interest. Briefly, samples were run on 8-16% SDS gradient gels and transferred to PVDF membranes. The membranes were probed with antibodies against eEF1A2 (1:500) (Proteintech, Cat# 66806-1-IG), cofilin (1:500) (Invitrogen, cat# PA5-24628), and Folr1 (1:500) (GenScript, custom), diluted in 5% milk or bovine serum albumin (BSA) (Sigma-Aldrich, Cat# A31565G) in TBST. Complementary HRP secondary antibodies were incubated for 2 h at 23°C, followed by washes and addition of Pierce ECL 2 Western Blotting substrate (ThermoFisher, Cat #80196). Blots were imaged on the ChemiDoc MP Imaging System (Bio-Rad, Hercules CA). Gapdh staining was used as loading control for lysate and flow-through samples.

Measurement of axon density in Folr1-deficient embryonic spinal cord explants

Embryonic spinal cord explants were isolated from stage 23 (24.75 hpf) embryos and transferred to Matrigel-coated glass bottom culture dishes containing saline culture medium, as described above. Vivo-morpholinos (Folr1 v-MO or Control v-MO) were added to saline culture medium 2 h after plating to a final concentration of 0.1-0.5 µM, and explants were grown for 18 h at 23°C. Samples were then fixed with 4% paraformaldehyde and immunostained as detailed above. Primary antibodies used: anti-Folr1 (1:1,000; Genscript, custom), anti-βIII-tubulin (1:900; Millipore, Cat# AB9354), and anti-acetylated α-tubulin

(1:2,000; Santa Cruz, Cat# SC-23950). Secondary antibodies used: Alexa Fluor 647 donkey anti-mouse, 1:500 (Life Technologies, Cat# A31571); Alexa Fluor 568 donkey anti-rabbit, 1:500 (Life Technologies, Cat# A10042); Dylight 405 donkey anti-chicken, 1:400 (Jackson ImmunoResearch, Cat# 703-475-155). Alexa Fluor 488-Phalloidin (Life Technologies, Cat# A12379) was used to label fibrillar actin. Samples were imaged on an inverted Nikon Eclipse T*i*2 C2 confocal microscope with the 10x air objective. Images were analyzed with NIS-Elements software (Nikon Instruments Inc., Melville NY) using the binary threshold and ROI selection tools in the βIII-tubulin-immunolabeled channel to obtain the Binary Area Fraction within the ROI, with ROIs drawn to exclude the explant cell body region from measurement.

Sholl analysis (Sholl, 1953) was performed using the Simple Neurite Tracer (SNT) plug-in (Ferreira et al., 2014) for Image J/Fiji (Schindelin et al., 2012). βIII-tubulin immunolabeling was used for axon tracing and subsequent Sholl analysis. Axons in each image were traced using the SNT 'trace' function, with a ring radius of 10 μm applied for Sholl analysis. Intersection data generated from radii falling within the explant cell body region were excluded from analysis.

Imaging and analysis of axon growth in Folr1-deficient embryonic spinal cord explants

Embryonic spinal cord explants from stage 23 embryos (24-24.75 hpf) were isolated and plated in Matrigel-coated glass bottom culture dishes as described above. Explants were grown for 3-4 h at 23°C. Vivo-morpholino (0.25 μM and 0.2 μM of Folr1 v-MO or Control v-MO) or vehicle (saline culture medium) was added to saline culture medium immediately prior to imaging. Time-lapse recordings were taken on an Olympus IX71 inverted microscope using the 10x air objective, with images taken every 15 min for 12 h. Recordings were then analyzed with Image J/Fiji software (Schindelin et al., 2012) using the MTrackJ plug-in (Meijering et al., 2012). Axon growth was measured by tracking the growth cone of each axon. The growth rate of each axon was represented as the "Distance to Reference point" (D2R) measurement data for each time point, using the starting point of the trace as the reference point. For retracting axons, the D2R

measurements were made negative from the point at which the axon retracted beyond its original starting point.

Tubulin distribution analysis in embryonic spinal cord axons

Embryonic spinal cords were isolated from stage 22-23 embryos (24-24.75 hpf), sectioned into explants, and plated on Matrigel-coated glass bottom culture dishes in saline culture medium, as detailed above. Vivo-morpholinos (Folr1 v-MO or Control v-MO) were added to saline culture medium 1 h after plating to a final concentration of 0.2 μM, and explants were grown for 18 h at 23°C. Samples were then fixed and immunostained as described above. Primary antibodies used: anti-acetylated α-tubulin, 1:2,000 (Santa Cruz, Cat# SC-23950); anti-tyrosinated α-tubulin, 1:1,000 (Millipore, Cat# MAB1864-I); anti-βIII-tubulin, 1:900 (Millipore, Cat# AB9354). Secondary antibodies used: Alexa Fluor 647 donkey anti-mouse, 1:500 (Life Technologies, Cat# A31571); Alexa Fluor 594 donkey anti-rat, 1:500 (Life Technologies, Cat# A21209); Dylight 405 donkey anti-chicken, 1:400 (Jackson ImmunoResearch, Cat# 703-475-155). Alexa Fluor 488-Phalloidin (Life Technologies, Cat# A12379) was used to label fibrillar actin as a reference for growth cone location. Samples were imaged on an inverted Nikon Eclipse T*i*2 C2 confocal microscope with the 10x air objective, and the 'large image' acquisition setting was used when necessary to capture the entirety of larger explants. Images were analyzed with NIS-Elements software (Nikon Instruments Inc., Melville NY). Analysis of protein distribution was performed using the 'Intensity Profile' tool and restricted to the distal-most 100 μm of the axon, beginning in the growth cone and extending proximally towards the soma.

Analysis of growth cone morphology in embryonic spinal cord axons

Embryonic spinal cords were isolated from stage 22-23 embryos (24-24.75 hpf), sectioned into explants, and plated on Matrigel-coated glass bottom culture dishes in saline culture medium, as detailed above.

Vivo-morpholinos (Folr1 v-MO or Control v-MO) were added to saline culture medium 1 h after plating to a final concentration of 0.2 μM, and explants were grown for 7-8 h at 23°C. Samples were then fixed with 4% paraformaldehyde and immunostained as described above. Primary antibodies used: anti-βIII-tubulin, 1:900 (Millipore, cat# AB9354). Secondary antibodies used: Dylight 405 donkey anti-chicken, 1:400 (Jackson ImmunoResearch, Cat# 703-475-155). Alexa Fluor 488-Phalloidin (Life Technologies, Cat# A12379) was used to label fibrillar actin. Samples were imaged on an inverted Nikon Eclipse T*i*2 C2 confocal microscope with the 60x oil immersion objective. Maximum intensity projections from z-stack optical sections spanning 10-15 μm were analyzed in NIS-Elements software (Nikon Instruments Inc., Melville NY). Growth cone area was determined by tracing an ROI encompassing filopodia and lamellipodia structures on the distal end of the axon shaft, where staining intensity of βIII-tubulin decreased sharply and phalloidin 488 staining intensity increased. Area and F-actin mean fluorescence intensity were measured from the growth cone ROIs for Control and Folr1 v-MO treated samples. The number of filopodia per growth cone was counted manually for each growth cone.

Analysis of eEF1A2 distribution in embryonic spinal cord axons

Embryonic spinal cords were isolated from stage 22-23 embryos (24-24.75 hpf), sectioned into explants, and plated on Matrigel-coated glass bottom culture dishes in saline culture medium, as detailed above. Vivo-morpholinos (Folr1 v-MO or Control v-MO) were added to saline culture medium 1 h after plating to a final concentration of 0.2 μM, and explants were grown for 7-8 h at 23°C. Samples were then fixed with 4% paraformaldehyde and immunostained as described above. Primary antibodies used: anti-eEF1A2, 1:3,000 (Proteintech, Cat# 66806-1-IG); anti-phospho eEF1A2 (Ser^{358}), 1:700 (Invitrogen, Cat# PA5-35404); and anti-βIII-tubulin, 1:900 (Millipore, Cat# AB9354). Secondary antibodies used: Alexa Fluor 647 donkey anti-mouse, 1:500 (Life Technologies, Cat# A31571); Alexa Fluor 568 donkey anti-rabbit, 1:350 (Life Technologies, Cat# A10042); Dylight 405 donkey anti-chicken, 1:400 (Jackson ImmunoResearch, Cat# 703-475-155). Alexa Fluor 488-Phalloidin (Life Technologies, Cat# A12379) was

used to label fibrillar actin. Samples were imaged on an inverted Nikon Eclipse T*i*2 C2 confocal microscope with the 60x oil immersion objective. Maximum intensity projections from z-stack optical sections spanning 10-15 μm were analyzed in NIS-Elements software (Nikon Instruments Inc., Melville NY) for eEF1A2 and phospho-eEF1A2 immunolabeled fluorescence intensity distribution. An ROI was drawn around the growth cone of each axon, as well as an ROI along the axon shaft. Growth cone area was determined as the point where staining intensity of βIII-tubulin decreased sharply towards the distal end of the axon shaft, and where phalloidin 488 staining intensity increased and filopodia and lamellipodia structures were well-defined. Binary thresholding was then applied to images of eEF1A2- and phospho-eEF1A2-immunolabeled samples. Mean fluorescence intensity measurements for the growth cone and shaft ROIs were graphed for each protein of interest, as well as the ratio between growth cone over shaft mean intensity.

Measurement and analysis of F-Actin dynamics in embryonic spinal cord axons

Time-lapse recordings of LifeAct-eGFP expressing axons in Folr1 v-MO and Control v-MO treated explants were acquired as detailed above. Kymographs from individual growth cones were generated using the Kymograph tool in the Tracking Analysis menu of NIS-Elements software. To create the kymographs, a 1-pixel-wide line was drawn beginning in the center of the growth cone and extending outward in the direction of filopodia growth. An ROI was then drawn to include the region corresponding to the actin structures outside the growth cone, and excluding pixels from actin within the growth cone, delineated by a bright border in the kymograph. Binary thresholding was then applied, and the binary area was used to calculate the total area of actin movement in μm^2 in order to compare actin dynamics in control and Folr1-deficient growth cones and before and after addition of Cyto-D in Folr1 v-MO and Control v-MO treated samples.

Data Collection and Statistical Analysis

Every set of experiments was repeated a minimum of 3 times, with a minimum of 3 independent clutches of embryos. Analysis of statistical significance of differences observed between control and experimental samples was performed through the following tests: Paired and unpaired Student's *t*-test; one-sample two-tailed *t*-test; Mann-Whitney *t*-test; one-way ANOVA; Brown-Forsythe and Welch ANOVA; and sixth order polynomial and Lorentzian-Cauchy linear regression models. Tests were chosen according to number of groups compared, data distribution, and experimental design. Results were considered significant when $p<0.05$. Statistical analyses were performed using GraphPad Prism software (GraphPad Software, Boston MA).

RESULTS

Knockdown of Folr1 affects axon behavior and morphology during growth

Folate receptor 1 (Folr1), one of the folate uptake systems present in neural tissue, is necessary for the formation of the neural tube, a process that occurs early in nervous system development in which the flat neural plate bends and folds inward to become the neural tube. Deficiency of Folr1 in developing mouse (Piedrahita et al., 1999) and frog (Balashova et al., 2017) embryos leads to neural tube defects because of the failure of the neural tube to form and close. Whether Folr1 has a role in later stages of neural development has not yet been explored.

To investigate the role of Folr1 after neural tube closure, when embryonic spinal cord neurons start to differentiate and elaborate axons, I first examined Folr1 expression in differentiating neurons. I excised the posterior neural tube from *Xenopus laevis* embryos and grew neural tube explants *in vitro* in Matrigel-coated culture dishes for 18 h in a saline culture medium. Immunostaining for Folr1 and cytoskeletal proteins shows that Folr1 is present in developing axons (**Fig. 3**). I then assessed the effect of knocking down Folr1 expression on axon outgrowth and morphology. To bypass the period of neural tube formation I incubated embryonic spinal cord explants with a cell permeant vivo-morpholino (Folr1 v-MO). A standard control vivo-morpholino (Control v-MO) served as control for these experiments. Western blot assays show that incubation of embryonic spinal cord explants with 0.2 μM Folr1 v-MO for 18 h effectively reduced Folr1 protein levels by 50% (**Fig. 4 A,B**). Immunostaining of embryonic spinal cord explants incubated with 0.2 μM Folr1 v-MO and Control v-MO for 18 h and stained for Folr1 shows that the reduced level of Folr1 protein is also apparent in the axons of Folr1 v-MO treated samples (**Fig. 4 C**). To assess the effect of Folr1 knockdown on axon growth and morphology I incubated *X. laevis* embryonic spinal cord explants with 0.1-0.5 μM Folr1 v-MO or Control v-MO for 18 h and then processed samples for immunofluorescence confocal imaging (**Fig. 5A**). Both Sholl analysis (**Fig. 5 B**) and binary thresholding (**Fig. 5 C-F**) were used to evaluate axon growth, the results of which indicate a Folr1 v-MO dose-dependent

reduction in axon length and density (**Fig. 5 D**). Based on this dose-dependent effect (**Fig. 5 B,D**), I chose 0.2-0.25 µM (**Fig. 5 E,F**) as the optimal concentration range of Folr1 v-MO and Control v-MO for subsequent experiments.

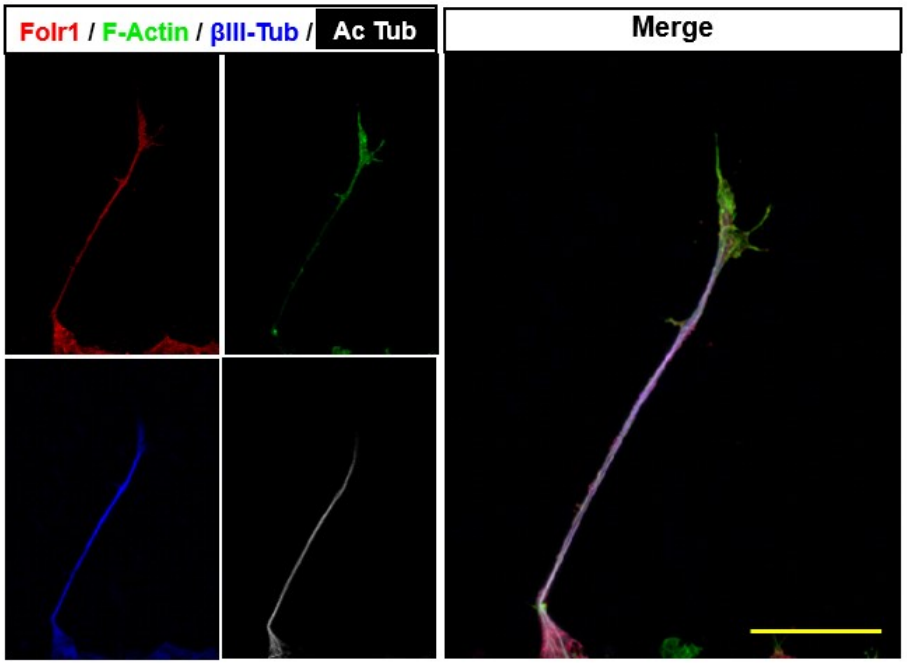

Figure 3. Folr1 localization in embryonic spinal cord neuron axons. Embryonic spinal cord explants isolated from neural tube stage embryos (stage 23) were plated on Matrigel, grown overnight, and processed for immunostaining of Folr1, βIII-tubulin (βIII-Tub), acetylated α-tubulin (Ac Tub), and F-actin. Representative immunofluorescence maximum intensity projection confocal image showing localization of Folr1 and cytoskeletal proteins in axons. Scale bar: 20 µm.

To further examine the Folr1 knockdown axonal phenotype, I performed time-lapse imaging of embryonic spinal cord explants incubated with either 0.25 µM Control v-MO, 0.2-0.25 µM Folr1 v-MO, or vehicle (saline**; Fig. 6 A**). Axon tracking data from these recordings show that the reduced axonal length and density exhibited by spinal cord explants deficient in Folr1 correlate with a higher occurrence of axon retraction in Folr1 v-MO treated samples. This retraction behavior was observed in 57% and 73% of axons treated with 0.2 or 0.25 µM Folr1 v-MO, respectively, whereas only 9% of axons retracted in 0.25 µM Control v-MO-treated samples (**Fig. 6 A,B**). Axon growth rate up to the point when axons retract is comparable in Folr1 v-MO- and Control v-MO-treated samples (**Fig. 6 A**). These results suggest that the

decrease in length and density in Folr1-deficient axons is due to the high incidence of retraction behavior rather than a slowdown of their growth.

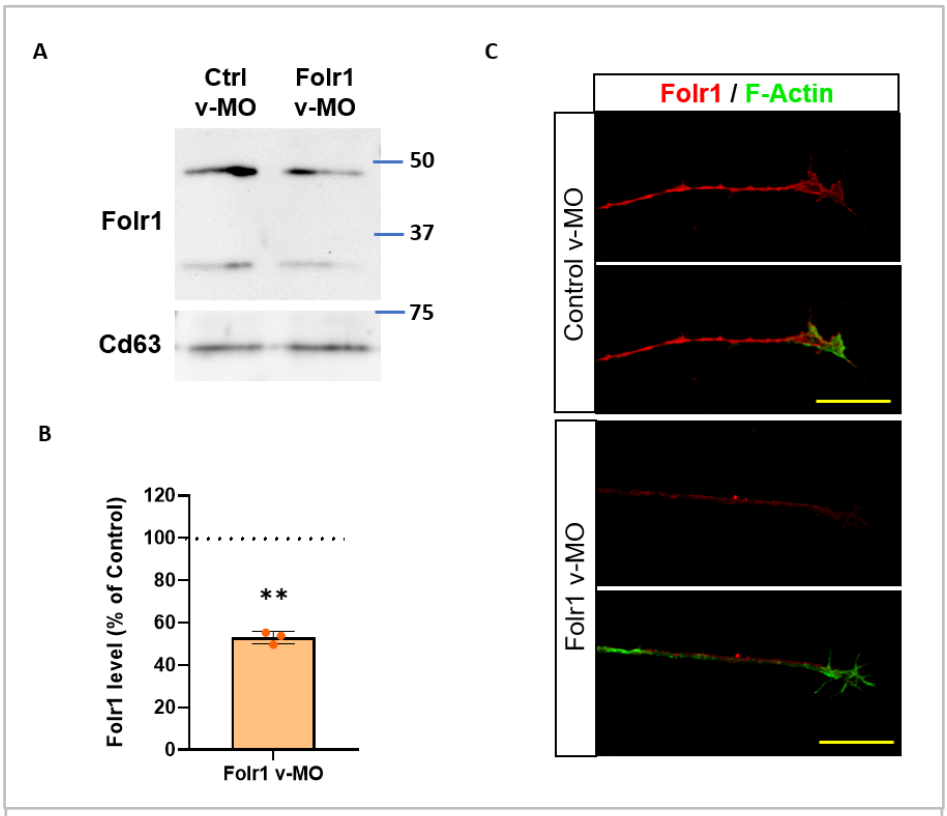

Figure 4. Knockdown of Folr1 expression *ex vivo*. Embryonic spinal cord explants were isolated from neural tube stage (stage 23) embryos, plated on Matrigel-coated glass bottom culture dishes, and treated with 0.20 µM Folr1 v-MO or Control v-MO (Ctrl v-MO) for 18 h. **A)** Representative Western blot assay immunoprobed for *Xenopus laevis* Folr1 and Cd63 as loading control. **B)** Graph shows individual data and mean±SD Folr1 band intensity in 0.2 µM Folr1 v-MO-treated samples relative to 0.2 µM Control v-MO samples (100%, dashed line). N=3 experiments; **p<0.05, one-sample two-tailed *t*-test, compared to hypothetical value 100%. **C)** Representative immunofluorescence confocal images showing reduced Folr1 fluorescence intensity in Folr1 v-MO treated axons. F-actin staining included to show location of growth cone. Scale bar: 20 µm.

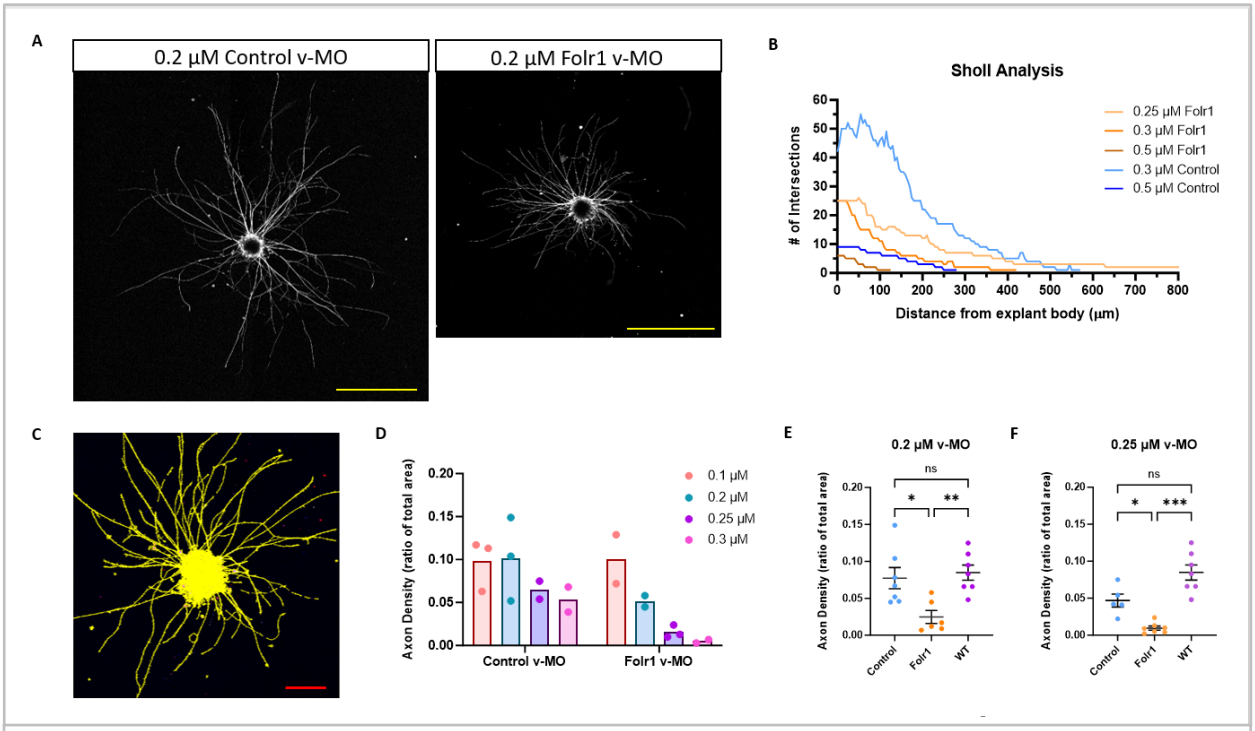

Figure 5. Folr1 knockdown decreases axon density. Embryonic spinal cord explants isolated from neural tube stage (stage 23) embryos were plated on Matrigel, v-MOs added 2 h after plating, grown overnight, and processed for immunostaining of acetylated α-tubulin. **A)** Representative immunofluorescence confocal images of acetylated α-tubulin labeling in explants incubated with 0.2 µM Control and Folr1 v-MO. Scale bar: 500 µm. **B)** Sholl analysis of axons from explants incubated with 0.25-0.5 µM Folr1 v-MO, in comparison to Control v-MO. **C)** Representative image of binary thresholding of βIII-tubulin labeling in immunostained embryonic spinal cord explants. Scale bar: 200 µm. **D)** Shown are individual and mean (bars) axon density (ratio of labeled area over total image area) from control and experimental groups, as indicated. **E-F)** Shown are individual and mean±SEM axon density (ratio of labeled area over total image area) from control and experimental groups, as indicated. In (**E**) n=6 from N=3 experiments; one-way ANOVA, *p=0.0154; **p=0.006; ns= not significant. In (**F**) n≥5 from N=3 experiments. Brown-Forsythe and Welch ANOVA, *p=0.0253; ***p=0.0006; ns= not significant.

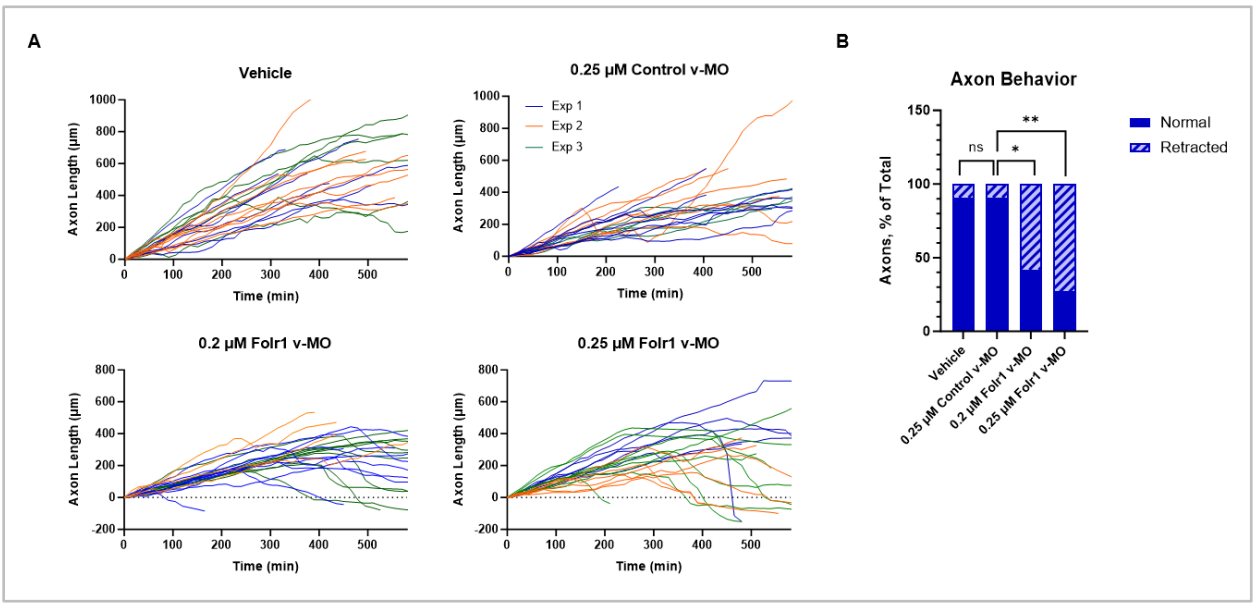

Figure 6. Retraction of developing Folr1-deficient axons. Embryonic spinal cord explants were plated on Matrigel-coated dishes and either 0.25 μM Control v-MO, 0.2 μM Folr1 v-MO, 0.25 μM Folr1 v-MO, or vehicle (saline) was added 4-5 h after plating. Time-lapse recordings of axon growth were taken with an Olympus inverted microscope 10x air objective for a duration of 12 h, with images taken every 15 min. **A)** Shown are tracings from individual axons from 3 time-lapse recordings from each experimental group, with one color for each experiment (Exp) represented. Negative axon length indicates axon retraction beyond the starting point of the trace. **B)** Data is represented as percent of total axons analyzed per group that either retracted or exhibited steady growth (Normal) during recording. Vehicle n=23; 0.25 μM Control v-MO n=23; 0.2 μM Folr1 v-MO n=26; 0.25 μM Folr1 v-MO n=26; from N=3 experiments per group. One-way ANOVA, *p<0.05; **p<0.01; ns= not significant.

Effect of Folr1 knockdown on cytoskeletal proteins

Following these findings of reduced axon length and density in Folr1-deficient axons, I was interested in exploring the effect of Folr1 knockdown on axonal microtubules. Microtubule dynamics and their overall structural integrity are important for proper axon growth. To examine the organization and structure of microtubules in Folr1-deficient axons I immunostained 0.2 μM Folr1 v-MO- and Control v-MO-treated embryonic spinal cord explants for acetylated (Ac) α-tubulin, tyrosinated (Tyr) α-tubulin, and βIII-tubulin. I chose to focus on acetylated and tyrosinated α-tubulin due to their proposed involvement in axon growth and neuronal development; α-tubulin acetylation is a post-translational modification mostly found in stable microtubules (Cambray-Deakin & Burgoyne, 1987; Li & Yang, 2015), while tyrosination is mostly found in dynamic regions of growing axons (Baas & Black, 1990; Sanyal et al., 2023). I restricted my analysis of tubulin distribution to the most distal 100 μm of the axon because this was where Tyr α-tubulin was primarily localized. Data show that within this region, the mean fluorescence intensity of βIII-tubulin is reduced in Folr1-deficient axons (**Fig. 7 A,B**). Mean fluorescence intensities of Ac and Tyr α-tubulin were not significantly different between control and Folr1-deficient axons (**Fig. 7 A,D**). Relative comparison between Tyr and Ac α-tubulin mean fluorescence intensity indicates no significant differences in distal regions of growing axons deficient in Folr1 compared to control axons (**Fig. 7 C,D**). These results suggest that Folr1 depletion affects overall microtubule density without affecting post-translational modifications; therefore, the defective microtubules in Folr1-deficient axons may be a secondary phenotype to an earlier target of the axonal architecture.

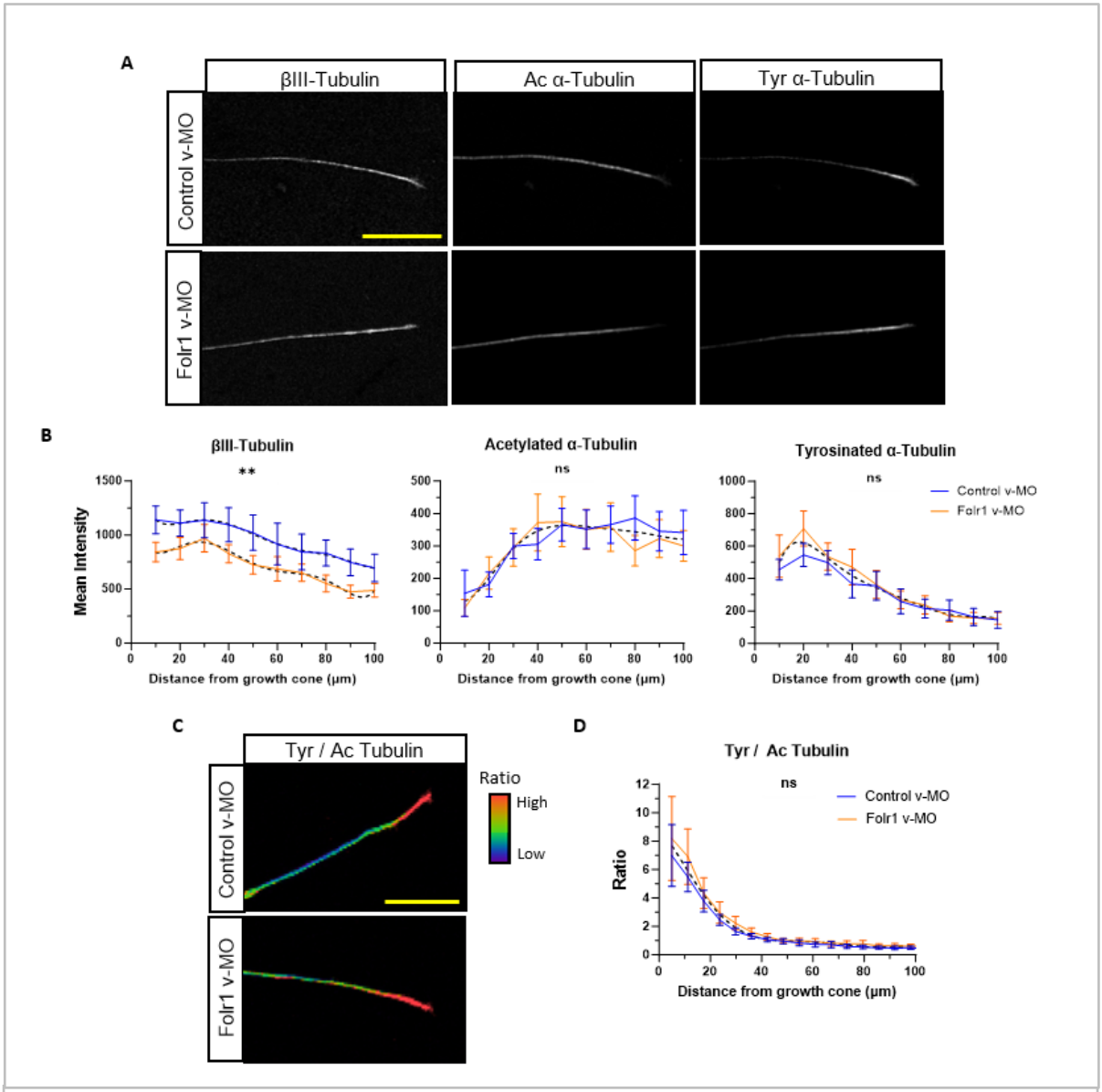

Figure 7. Folr1 knockdown decreases microtubule density in axons without affecting microtubule stability. Embryonic spinal cord explants were isolated from neural tube stage (stage 23) embryos, plated on Matrigel-coated glass bottom culture dishes, and incubated in 0.2 μM Folr1 v-MO or Control v-MO for 18 h. Explants were then processed for immunostaining for βIII-tubulin, tyrosinated (Tyr) α-tubulin, acetylated (Ac) α-tubulin, and F-actin. **A)** Representative immunofluorescence maximum intensity projection images of Tyr, Ac, and βIII-tubulin distribution in the distal region of axons in control and experimental samples. **B)** Shown are mean±SEM intensity profile data from immunofluorescence confocal images. Data were binned per every 10 μm for the most distal 100 μm of the axon shaft, starting in the growth cone (0, set by F-actin labeling). **C)** Representative image showing the ratio of Tyr over Ac tubulin immunolabeling fluorescence intensity along an axon in control and Folr1 v-MO samples. Heat-map shows red as the highest and purple as the lowest Tyr /Ac tubulin fluorescence intensity ratio. **D)** Shown are mean±SEM ratio of fluorescence intensity between Tyr and Ac tubulin. Data were binned per every 10 μm for the most distal 100 μm of the axon shaft, starting in the growth cone (0). n=24 for Folr1 v-MO axons and n=33 for Control v-MO axons, from N=6 explants from 3 experiments. A sixth order polynomial linear regression model was used to compare curves in (**B**) and (**D**); **p=0.0059; ns= not significant. 'Best fit' curve for each group is represented by a black dashed line. Scale bars: 50 μm.

During axon development, the coordinated action of actin and microtubule dynamics within the growth cone are vital for axon growth and pathfinding. Within the peripheral domain of the growth cone, the balance between actin polymerization and depolymerization drives advancement of the axon along the substrate. In current models of axon outgrowth, actin filaments in the peripheral domain are the primary downstream target of neurotrophic factors, and the resulting change in actin dynamics in turn affects microtubule activity in the central domain (Dent & Gertler, 2003; Letourneau, 2009). In order to explore the possible effect of Folr1 knockdown on actin dynamics before the axon retraction phenotype is apparent, I first assessed F-actin enrichment in growth cones of Folr1-deficient and control axons. To do so, I incubated embryonic spinal cord explants with 0.2 μM Folr1 or Control v-MO, allowed them to grow for 7-8 h, then processed samples for immunostaining. An earlier time point was chosen for fixation to better capture axons in an active state of growth, before growth cone collapse and axon retraction. Analysis of growth cone area and mean fluorescence intensity of F-actin in Folr1 v-MO and Control v-MO treated axons did not indicate any significant difference between groups (**Fig. 8 A,B**). The number of filopodia per growth cone in control and Folr1-deficient axons was also examined. Data indicate that the distribution of the number of filopodia is different for Folr1 v-MO samples compared to controls (**Fig. 8 C**). Whereas the majority of Control v-MO growth cones contain 5-10 filopodia, Folr1-deficient axons exhibited a wider range with comparatively few growth cones falling within the predominant filopodia range observed in controls. This may report on a more erratic behavior of growth cones deficient in Folr1.

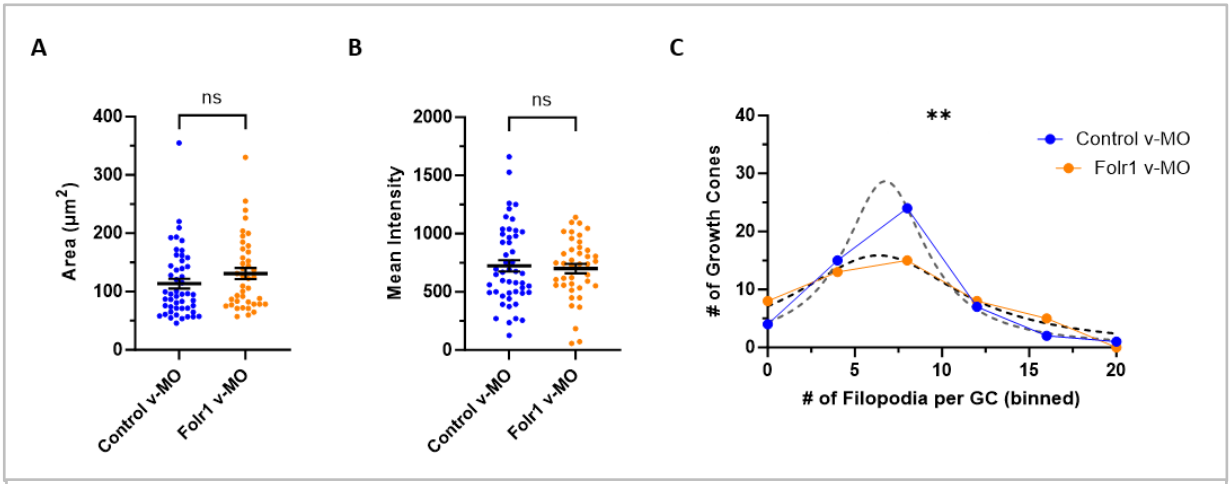

Figure 8. Growth cone morphology in Folr1-deficient axons. Embryonic spinal cord explants were isolated from neural tube stage (stage 23) embryos, plated on Matrigel-coated glass bottom culture dishes, treated with 0.2 µM Folr1 v-MO or Control v-MO, and grown for 8 h before processing for immunostaining and subsequent confocal imaging. **A)** Individual and mean±SEM area of growth cones in Folr1 v-MO and Control v-MO embryonic spinal cord axons. **B)** Individual and mean±SEM F-actin mean fluorescence intensity within growth cones from Folr1 v-MO and Control v-MO embryonic spinal cord axons. **C)** Number of filopodia per growth cone (GC) in Folr1 v-MO and Control v-MO embryonic spinal cord axons, binned. Collapsed growth cones were counted as having 0 filopodia. Unpaired t-test comparison in (**A**) and Mann-Whitney test in (**B**); Lorentzian Cauchy linear regression was performed for curve comparison in (**C**), with 'best fit' represented as dashed curves on graph. **p= 0.0054; ns= not significant. Folr1 v-MO n= 41 and Control v-MO n=49, from 5 experiments.

To further investigate the role of Folr1 in actin dynamics, I expressed in developing embryos the genetically-encoded actin dynamics reporter LifeAct-eGFP and timelapse imaged embryonic spinal cord explants obtained from these embryos, after incubating explants with 0.2 µM Folr1 or Control v-MO for 5-6 h (**Fig. 9 A**). Total area of actin movement, measured by kymographs of F-actin structures in the growth cones (**Fig. 9 B**) of control and Folr1 v-MO samples, did not show a significant difference (**Fig. 9 C**). Numerous compounds that affect actin dynamics have been identified, such as the actin destabilizing compounds cytochalasin D and latrunculin A, and actin stabilizing compounds such as jasplakinolide and phalloidin (Bubb et al., 1994; Goddette & Frieden, 1986; I. Spector et al., 1999). Actin filament turnover is essential to growth cone motility and axon guidance (Gomez & Letourneau, 2014; Lowery & Vactor, 2009), and treatment with actin stabilizing compounds causes axon retraction (Gallo et al., 2002). Indeed, addition of 0.5 µM jasplakinolide to cultured embryonic spinal cord axons caused growth cone collapse and retraction of axons within several minutes (n≥3). Thus, I chose to use Cyto-D in order to attempt to rescue the retraction behavior of Folr1-deficient axons. Axons were imaged every 20 s for a total of 15 min prior

to and after addition of 0.1 µM Cyto-D. Actin dynamics were assessed via kymograph in order to capture the movement of filopodia over time. Data show significant disruption of growth cone actin dynamics by Cyto-D in Control v-MO axons (**Fig. 9 D**). In contrast, in the background of Folr1-deficiency the effect of Cyto-D on actin dynamics is not apparent (**Fig. 9 D**), suggesting that the two treatments may counteract each other in their dysregulation of actin dynamics. Taken together, these results suggest that Folr1 is necessary for appropriate actin dynamics to promote axonal outgrowth.

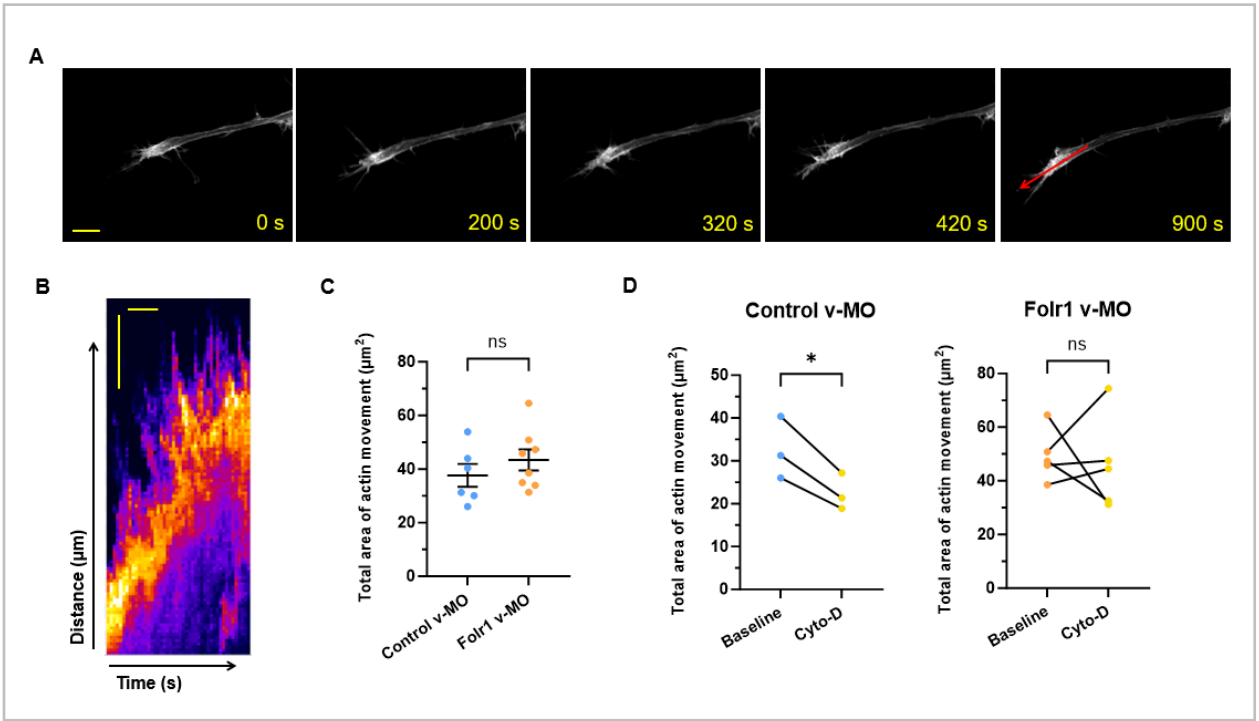

Figure 9. Actin dynamics in Folr1-deficient axons. Embryonic spinal cord explants were isolated from neural tube stage (stage 23) LifeAct-eGFP expressing embryos, plated on Matrigel-coated glass bottom culture dishes, treated with 0.2 µM Folr1 v-MO or Control v-MO and grown for 5-6 h prior to imaging. Time-lapse recordings of axons were taken every 20 s for a total of 15 min on an inverted confocal microscope with a 60x oil objective. **A)** Representative images of an axon from a control time-lapse recording. Red arrow indicates line probe positioning for kymographs. Scale bar: 10 µm. **B)** Representative kymograph projection from the axon in (**A**) showing F-actin activity. Time (s) is represented on the X-axis, and distance along the probe is represented on the Y-axis (µm). Y-axis scale bar: 5 µm; X-axis scale bar: 200 s. **C-D)** Kymograph analysis of F-actin activity in LifeAct-eGFP expressing embryonic spinal cord axons incubated with 0.2 µM Control or Folr1 v-MO. Data in **(C)** are individual and mean±SEM of actin dynamics in growth cones from each group, represented as total area of actin movement in μm^2. Control v-MO n=6 and Folr1 v-MO n=7, from N≥3 experiments. Unpaired *t*-test, ns= not significant. Data in **(D)** is represented as a pairwise comparison of actin dynamics in axons before (Baseline) and after addition of 0.1 µM cytochalasin-D (Cyto-D). Control v-MO n=3 and Folr1 v-MO n=4, from N≥3 experiments. Paired *t*-test, *p= 0.029; ns= not significant.

Folr1 interacting proteins in growing axons

Based on previous mass spectrometry assays of Folr1 co-immunoprecipitated (co-IPed) embryo samples, several subunits of the eukaryotic elongation factor 1 complex were identified as interacting proteins with Folr1, including delta (eEF1Bδ), gamma (eEF1Bγ), and alpha (eEF1A), as well as cofilin. Both eEF1A2 (Carriles et al., 2021; Mendoza et al., 2021) and cofilin (Bamburg, 1999; Pavlov et al., 2007; Prochniewicz et al., 2005) are proteins that regulate actin dynamics. Thus, I chose to first investigate whether eEF1A2 interacts with Folr1. eEF1A2 is highly conserved across species, and is expressed in neural tissue past neurulation stages in *X. laevis* (Djé et al., 1990; Krieg et al., 1989). I performed co-IP assays with neural tissue isolate from WT embryos, followed by Western blot assays of the resulting IP samples. Since the custom Folr1 antibody used was raised in rabbit, normal rabbit IgG was used as a control. Western blot assays show a strong band corresponding to eEF1A2 in Folr1-IP samples, thus indicating that Folr1 and eEF1A2 do indeed interact in the developing neural tube (**Fig. 10 A**). Conversely, despite testing several conditions with multiple IP samples, a band positive for cofilin in Folr1-IP samples was not observed (**Fig. 10 A**). I then assessed eEF1A2 localization in axons by immunostaining embryonic spinal cord explants. eEF1A2 is present and staining is fairly uniform throughout the axon and growth cone. A merge between max intensity projection images and an orthogonal view of a single frame of eEF1A2 and Folr1 immunostaining indicates that eEF1A2 colocalizes with Folr1 throughout the shaft and growth cone of axons (**Fig. 10 B,C**).

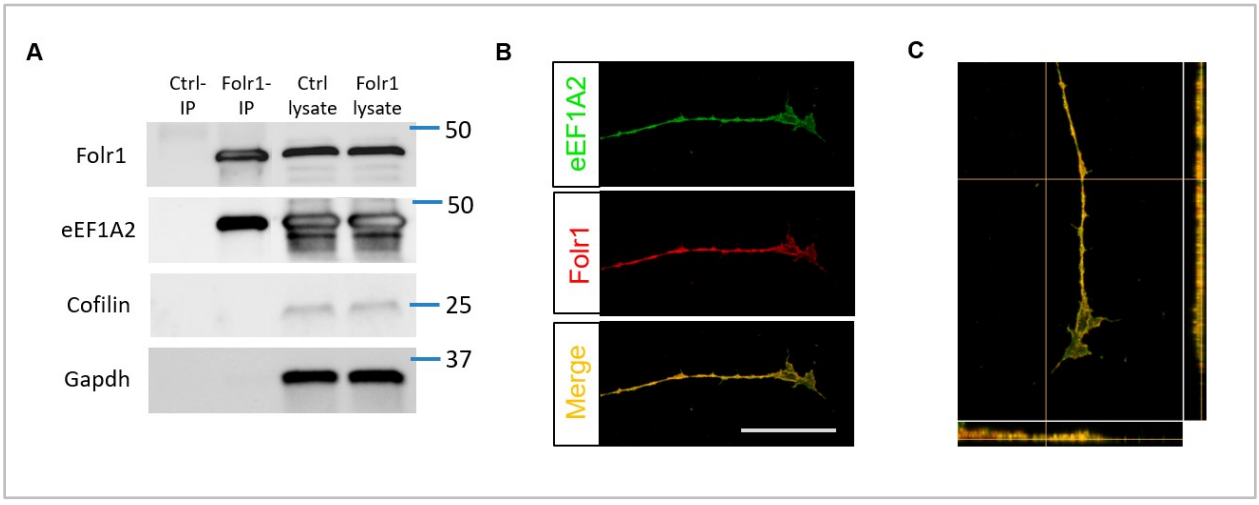

Figure 10. eEF1A2 interacts with Folr1. A) A co-immunoprecipitation (co-IP) assay was performed with neural tissue-enriched lysates from wild-type embryos. Lysates were incubated with anti-Folr1-crosslinked (Folr1-IP) and anti-Rabbit IgG-crosslinked (control, Ctrl-IP) beads. Co-IPed proteins were dissociated from beads and resolved on SDS-PAGE gels for Western blot assay with anti-Folr1 and anti-eEF1A2 antibodies. Shown is a representative Co-IP/Western blot assay that was repeated 4 times with similar results. **B)** Embryonic spinal cord explants were isolated from neural tube stage (stage 23) embryos, plated on Matrigel-coated glass bottom dishes, and incubated with Control v-MO for 8 h. Explants were then processed for immunostaining for eEF1A2 and Folr1. Shown are representative maximum fluorescence intensity confocal images demonstrating overlap in localization of eEF1A2 and Folr1 in Control v-MO axons. Scale bar: 25 µm. **C)** Orthogonal view of a single frame from the confocal image in (**B**) demonstrating colocalization of eEF1A2 and Folr1.

To determine whether eEF1A2 axonal localization is dependent on Folr1, I treated embryonic spinal cord explants with 0.2 µM Folr1 v-MO or Control v-MO. For these experiments I chose to fix the samples at an earlier time point (7-8 h) to capture Folr1-deficient axons in an active state of growth, prior to growth cone collapse and retraction. Results show that in Folr1-deficient axons the mean fluorescence intensity of eEF1A2 is lower in both axon shaft and growth cone and enrichment at the growth cone is significantly reduced (**Fig. 11 A-D**). I also examined the distribution of phospho(Ser^{358})-eEF1A2 in immunostained embryonic spinal cord explants. Phosphorylation at Ser^{358} has been shown to alter F-actin binding and 'turn off' the protein elongation function of eEF1A2 (Mendoza et al., 2021). Analysis of phospho-eEF1A2 in 0.2 µM Folr1 v-MO and Control v-MO treated embryonic spinal cord axons indicates a reduction in the mean intensity of immunofluorescence staining in both the axon shaft and growth cone (**Fig. 11 E-G**). Comparison between growth cone and shaft mean intensity staining for phospho-eEF1A2 did not indicate a significant difference (**Fig. 11 H**). Overall, my results indicate that Folr1 and eEF1A2 interact, and that Folr1 knockdown alters protein level and localization of eEF1A2 in axons. In turn, depletion of eEF1A2 in growth cones of Folr1-knockdown samples may result in altered actin dynamics, arrested axon growth and axon retraction.

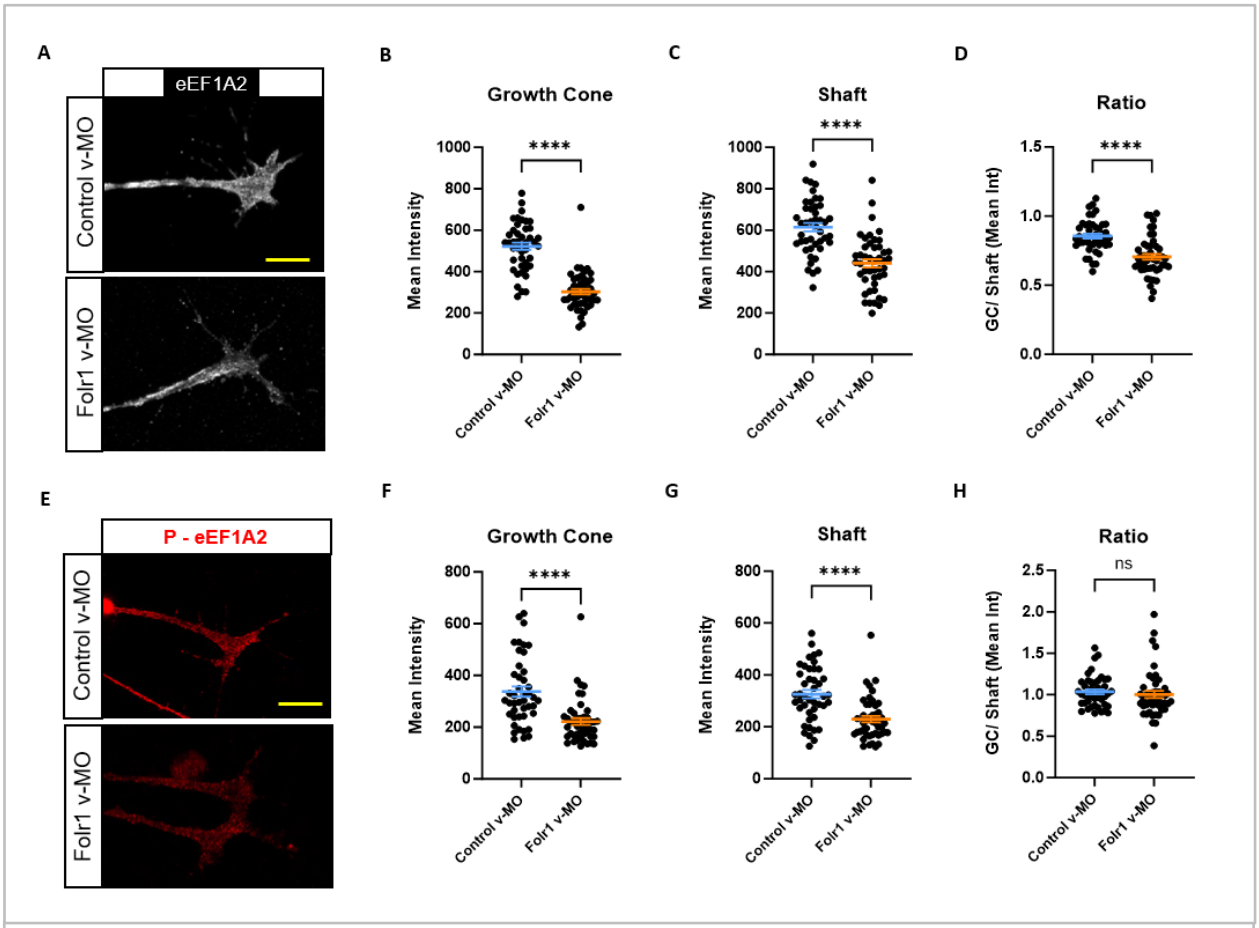

Figure 11. Folr1 knockdown results in depletion of eEF1A2 and phospho-eEF1A2 in axons. Embryonic spinal cord explants were isolated from neural tube stage (stage 23) embryos, plated on Matrigel-coated glass bottom dishes, and incubated with 0.2 μM Folr1 v-MO or Control v-MO for 8 h. Explants were then processed for immunostaining for eEF1A2, phospho-eEF1A2, βIII-tubulin, and F-actin. **A)** Shown are representative confocal images demonstrating reduced staining intensity of eEF1A2 in Folr1-deficient axons. **B-D)** Individual and mean±SEM eEF1A2 fluorescence intensity in axonal growth cone (GC, **B**) and shaft **(C)** and GC/shaft ratio **(D)** in Control v-MO and Folr1 v-MO treated explants. **E)** Representative confocal images demonstrating reduced immunostaining of phospho-eEF1A2 (P-eEF1A2) in Folr1 v-MO deficient axons. **F-H)** Individual and mean±SEM phospho-eEF1A2 fluorescence intensity in axonal growth cone (GC, **F**) and shaft **(G)** and GC/shaft ratio **(H)** in Control v-MO (n= 44) and Folr1 v-MO (n= 46) treated explants, from N=3 experiments. Mann-Whitney *t*-test, ****p<0.0001; ns= not significant. Scale bars: 10 μm.

DISCUSSION

My investigation demonstrates a role for Folr1 in axon outgrowth of differentiating spinal cord neurons in *Xenopus laevis* embryos. My findings show that Folr1 localizes to the axons of embryonic spinal cord neurons and interacts with potential regulators of cytoskeletal protein dynamics, prominently with eEF1A2, an elongation factor complex subunit that has recently been identified as a regulator of actin dynamics and neuronal morphology.

Previous studies from our lab and others identified Folr1 expression in the neural plate. Transcripts of folr1 are detected in the neural folds of mouse embryos (Piedrahita et al., 1999) and its protein localizes to the apical membrane of superficial neural plate cells in *Xenopus laevis* embryos during neural plate folding (Balashova et al., 2017). My findings indicate that expression of Folr1 persists in differentiating neurons and localizes not only to the cell body but also throughout growing axons. Similarly, it has been shown in an adult rat model of sciatic nerve injury that Folr1 is expressed in the injured axon and addition of folate promotes axon regeneration in a Folr1-dependent manner (Iskandar et al., 2010).

Folr1 is a glycosylphosphatidylinositol (GPI)-anchored protein (Luhrs & Slomiany, 1989). According to current research, GPI-anchored proteins are localized to lipid rafts, which are distinct compartments of the exoplasmic leaflet of the lipid bilayer primarily consisting of cholesterol and sphingolipids (Simons & Ikonen, 1997; Simons & Toomre, 2000). Although not definitive, there is strong evidence to support the idea that Folr1 is localized to lipid rafts (Sabharanjak & Mayor, 2004). Folr1 was shown to localize to specific sub-micron sized domains in membranes in a GPI-anchor and cholesterol-dependent manner in Chinese hamster ovary (CHO) cells expressing Folr1 constructs (Friedrichson & Kurzchalia, 1998; Varma & Mayor, 1998). Numerous signaling molecules, receptors, and ion channels are associated with or localized to lipid rafts, potentially to facilitate interaction of these proteins and trigger signaling pathways for specific downstream effects (Tsui-Pierchala et al., 2002). In neurons, lipid rafts are

involved in neurotrophic signaling (Encinas et al., 2001; Tansey et al., 2000), axon guidance (Walsh & Doherty, 1997), cellular adhesion (Davy et al., 1999; Kasahara et al., 2000; Walsh & Doherty, 1997), and synaptic transmission and plasticity (Brusés et al., 2001; Martens et al., 2000). Thus, the association of Folr1 to lipid rafts opens up exciting possibilities for interactions with cytoskeleton-associated proteins and signaling pathways.

The presence of Folr1 in axons argues for a specific role in this subcellular compartment. I discover that Folr1 is necessary for the steady outgrowth of developing axons during the early stages of neuronal morphogenesis. Folr1 acting as a regulator of changes in cell morphology is also apparent in neural plate cells, where Folr1 *de novo* synthesis and apical localization are necessary for the developmentally timed apical constriction of these cells during neural plate folding (Balashova et al., 2017). Similarly, in epithelial cell cultures, folate/Folr1 rescue the function of the Rho-kinase binding deficient mutant of Shroom3 by recruiting myosin light chain kinase- and Src-kinase-dependent mechanism to enable apical constriction (Martin et al., 2019).

The tip of a developing axon, known as the growth cone, represents the leading edge of the neuronal process where cytoskeletal proteins dynamically assemble and disassemble to allow for oriented outgrowth of the axon towards the target cell. The specific structure that the growth cone adopts is important for achieving the appropriate rate of outgrowth and exploration and response to environmental cues (Dent et al., 2011; Dent & Gertler, 2003; Letourneau, 2009). The number of filopodia and lamellipodia structures, as well as overall growth cone morphology, varies throughout development in different cell types and substrates (Bovolenta & Mason, 1987; Letourneau, 1979; Nordlander, 1987). For example, in *in vivo* studies exploring axon pathfinding and growth cone morphology in the developing cerebral cortex of hamster pups (Kalil, 1996) and optic tract of mouse embryos (Bovolenta & Mason, 1987), growth cones had more filopodia and lamellipodia projections and were generally more spread out while exploring the extracellular environment, but adopted an overall more conical streamlined shape with fewer filopodia and lamellipodia projections when closer to their target. The ability of the axon to respond appropriately to trophic factors

and chemoattractant and repulsive cues is also closely tied to growth cone morphology and is thus crucial for pathfinding and guidance of axons during central nervous system development (Connolly et al., 1985; Dent & Gertler, 2003; Tessier-Lavigne & Goodman, 1996). In my study, I found that the profile of the number of filopodia in growth cones of Folr1-deficient axons differed from that of control axons, suggesting that Folr1 is important for enabling the development of growth cone morphology suitable for proper axon outgrowth and pathfinding.

Hence, my findings, along with previous discoveries by our lab and others, point towards a Folr1-dependent regulation of cytoskeletal protein dynamics to enable changes in cell morphology and tissue morphogenesis. Our lab previously reported on interactions between Folr1 and cell adherens junction molecules, C-cadherin and β-catenin, in the folding neural plate (Balashova et al., 2017). This complex anchors the actomyosin contractile network to enable reduction of the apical surface of neural plate cells and bending of the neural plate. My investigation shows that Folr1 is necessary for appropriate density of axonal microtubules in the embryonic spinal cord. I also assessed whether acetylation and tyrosination of α-tubulin, post-translational modifications that confer increased stability or dynamism to axonal microtubules, respectively (Baas & Black, 1990; Brown et al., 1993; Webster & Borisy, 1989), are dependent on Folr1. The data reveal that the presence of these modified tubulins is not affected by the status of Folr1 expression. Nevertheless, microtubules are vital for the structural integrity of axons; thus, the necessity of Folr1 for providing appropriate microtubule density could be a mechanism by which Folr1 supports steady axonal outgrowth. Interestingly, there has been some debate in the literature about whether disruption of microtubules is sufficient to elicit axon retraction in a manner comparable to the behavior observed in Folr1-deficient axons. Some studies examining the effect of microtubules on axon growth show that treatment with microtubule-disrupting drugs results in axon retraction (Daniels, 1972; Yamada et al., 1970), while others have found that disrupting microtubules alone is not sufficient to elicit this response (Datar et al., 2019; Fan et al., 1993). Whether restoring βIII-tubulin levels in growing axons would rescue the retraction phenotype in Folr1-deficient axons remains to be explored.

Equally important for axon structure, and particularly for growth cone shape and function in developing neurons, is F-actin. Treatment of axons with the F-actin depolymerizing drug Latrunculin A causes growth cone collapse and retraction of the bulk of the axon along a retraction front while leaving behind a thin trail of membrane, a process that takes place over the course of several hours in dorsal root ganglion (DRG) cell cultures from chick embryos (Datar et al., 2019). Treatment with the F-actin stabilizing drug Jasplakinolide also induces growth cone collapse followed by axon retraction over the course of several minutes in retinal and DRG cells (Gallo et al., 2002), which is similar to the phenotype I observed during time-lapse recordings of control and Folr1-deficient embryonic spinal cord neuron axons treated with an F-actin stabilizing drug, indicating that disruption of actin dynamics leads to axon retraction. Interestingly, although Folr1 knockdown does not significantly alter actin dynamics in the growth cone, addition of the actin depolymerizing drug Cytochalasin-D (Cyto-D) in the background of Folr1 deficiency prevents the disruption in actin dynamics caused by this drug in control axons. Treatment with Cyto-D results in disruption of cytoskeletal organization and the production of actin foci by severing or otherwise disrupting the structure of actin filaments and inhibiting actin polymerization (Goddette & Frieden, 1986; Schliwa, 1982). The exact mechanisms through which Cyto-D severs actin filaments and inhibits polymerization are not yet known, although the prevailing theory is that Cyto-D binds to the barbed end of actin filaments to prevent further addition of G-actin monomers (Brenner & Korn, 1979; Casella et al., 1981; Schliwa, 1982), possibly in a Mg^{2+}-dependent manner also involving altered ATP hydrolysis activity (Goddette & Frieden, 1986). Taking this into account, a potential explanation for the altered Cyto-D activity in Folr1-deficient axons is that Folr1 deficiency may counteract the action of Cyto-D treatment on actin dynamics. Alternatively, the effect of Folr1 deficiency on actin dynamics may override the effect of Cyto-D, masking the observation of the changes in actin dynamics imposed by the drug.

This investigation identifies eEF1A2 as a Folr1-interacting protein and shows they colocalize in the growing axon. This elongation factor complex subunit has been shown to have numerous functions, one canonical of enabling protein synthesis and another as a regulator of actin dynamics. Although not specific

to the eEF1A2 isoform, eEF1A has been shown to interact with F-actin and β-actin mRNA in chicken embryo fibroblast and rat mammary adenocarcinoma cultures (Liu et al., 2002). In addition, altering residues on the actin binding domain of eEF1A and expression of this truncated form in yeast resulted in reduced actin binding and bundling *in vitro* and disturbed cytoskeletal organization *in vivo* (Gross & Kinzy, 2005). Moreover, Mendoza and colleagues (2021) found that expression of an eEF1A2 mutant modified to prevent phosphorylation at the Ser^{342}, Ser^{358}, Ser^{393}, and Ser^{445} residues on domain III resulted in reduced actin dynamics in HEK293T cells and reduced spine density in cultured hippocampal neurons from mouse embryos. Conversely, expression of a phospho-mimetic mutant modified at the same residues resulted in reduced interaction with F-actin but an increase in actin dynamics in dendritic spines of cultured hippocampal neurons. Additionally, expression of the phospho-null and phospho-mimetic eEF1A2 mutants in yeast shows impaired ability of the phospho-mimetic form to participate in protein translation, suggesting that phosphorylation at these sites regulates eEF1A2 function and may allow for coordination of protein translation and F-actin dynamics during dendritic spine remodeling in hippocampal neurons (Mendoza et al., 2021). eEF1A2 has also been shown to regulate filopodia production through its interaction with phosphatidylinositol-4 kinase III beta (PI4KIIIβ) and Cdc42 in experiments involving overexpression of eEF1A2 in BT549 breast carcinoma and Rat2 fibroblast cell lines (Jeganathan et al., 2008).

My findings show that eEF1A2 and phospho-eEF1A2 localization to axons and growth cones is dependent on Folr1 expression. Mutations in eEF1A2 are associated with neurodevelopmental disorders in humans (Lam et al., 2016; Nakajima et al., 2015). A well-studied loss of function mutation (*Wst*) in the eEF1A2 gene causes ataxia, axon retraction, muscle degeneration, and ultimately death by 4 weeks after birth in mice (Chambers et al., 1998; Shultz et al., 1982). The developmental timeline of the phenotype observed in *Wst* animals (Chambers et al., 1998; Shultz et al., 1982) closely aligns with the developmental stage I focus on in my study, during which neuronal differentiation and axon outgrowth occur in the embryonic spinal cord of *X. laevis* embryos (Taylor & Roberts, 1983).

Taken together, the interaction between Folr1 and eEF1A2 in developing axons and growth cones has exciting implications for localized regulation of protein synthesis and F-actin dynamics in growing axons and growth cones. Given the importance of folate, Folr1, and eEF1A2 for proper neural development, further investigations should focus on elucidating the molecular interactions and signaling mechanisms that orchestrate Folr1-dependent axon development.

CONCLUSION

To date, studies exploring the role of folate and Folr1 in neurodevelopment have largely focused on their role during neural tube formation. Whether Folr1 is involved in neural development beyond neurulation has remained unexplored. Thus, in my work I investigated the possible role of Folr1 in embryonic spinal cord development, and in particular axon growth. I show that Folr1 is expressed in axons during embryonic stages of spinal cord development, and that knocking down Folr1 expression results in retraction of growing axons. Upon further investigation, I find that βIII-tubulin is depleted and that filopodia production and actin dynamics are altered in the growth cones of Folr1-deficient axons. Additionally, I find that Folr1 interacts and colocalizes with eEF1A2, a GTP-binding protein whose canonical function is to facilitate the process of protein elongation as part of the protein synthesis machinery but has also been found to bind to and bundle F-actin and regulate filopodia production and F-actin dynamics. I show that Folr1 knockdown results in depletion of eEF1A2 and phospho-eEF1A2 in axons, and in particular, altered localization of eEF1A2 in growth cones. Taken together, my work highlights the importance of Folr1 for proper axon outgrowth and neural development.

Further investigation is needed to fully examine the mechanism through which Folr1 and eEF1A2 may regulate axon growth. In particular, whether depletion and altered localization of eEF1A2 in growth cones of Folr1-deficient axons has an impact on local protein synthesis remains to be explored. In addition, it is not yet known whether eEF1A2 depletion in the growth cone is solely responsible for the observed axon retraction behavior of Folr1-deficient axons or if other proteins or signaling pathways are involved in this response, particularly regarding the regulation of βIII-tubulin levels and F-actin dynamics in axons. Ultimately, my project has highlighted the importance of Folr1 for axon outgrowth during early stages of nervous system development, opening up exciting possibilities for future research endeavors.

REFERENCES

Abbott, C. M., Newbery, H. J., Squires, C. E., Brownstein, D., Griffiths, L. A., & Soares, D. C. (2009). eEF1A2 and neuronal degeneration. *Biochemical Society Transactions*, *37*, 1293–1297.

Abdallah, B., Hourdry, J., Krieg, P. A., Denis, H., & Mazabraud, A. (1991). Germ cell-specific expression of a gene encoding eukaryotic translation elongation factor 1 alpha (eEF-1 alpha) and generation of eEF-1 alpha retropseudogenes in Xenopus laevis. *Proceedings of the National Academy of Sciences of the United States of America*, *88*(20), 9277–9281. https://doi.org/10.1073/pnas.88.20.9277

Amiri, A., Noei, F., Jeganathan, S., Kulkarni, G., Pinke, D. E., & Lee, J. M. (2007). eEF1A2 activates Akt and stimulates Akt-dependent actin remodeling, invasion and migration. *Oncogene*, *26*(21), 3027–3040. https://doi.org/10.1038/sj.onc.1210101

Anand, N., Murthy, S., Amann, G., Wernick, M., Porter, L. A., Cukier, I. H., Collins, C., Gray, J. W., Diebold, J., Demetrick, D. J., & Lee, J. M. (2002). Gene encoding protein elongation factor EEF1A2 is a putative oncogene in ovarian cancer. *Nature Genetics*, *31*, 301–305. https://doi.org/10.1038/ng904

Antony, A. C. (1992). The biological chemistry of folate receptors. *Blood*, *79*(11), 2807–2820.

Antony, A. C. (1996). Folate Receptors. *Annu Rev Nutr*, *16*, 501–521.

Baas, P. W., & Black, M. M. (1990). Individual microtubules in the axon consist of domains that differ in both composition and stability. *The Journal of Cell Biology*, *111*(2), 495–509. https://doi.org/10.1083/jcb.111.2.495

Balashova, O. A., Visina, O., & Borodinsky, L. N. (2017). Folate receptor 1 is necessary for neural plate cell apical constriction during *Xenopus* neural tube formation. *Development*, *144*, 1518–1530. https://doi.org/10.1242/dev.137315

Bamburg, J. R. (1999). Proteins of the ADF/Cofilin family: Essential regulators of actin dynamics. *Annu Rev Cell Dev Biol*, *15*, 185–230.

Barry, D. M., Millecamps, S., Julien, J.-P., & Garcia, M. L. (2007). New movements in neurofilament transport, turnover and disease. *Experimental Cell Research*, *313*(10), 2110–2120. https://doi.org/10.1016/j.yexcr.2007.03.011

Baxter, M. G., Miller, A. A., & Webster, R. A. (1973). Some studies on the convulsant action of folic acid. *British Journal of Pharmacology*, *48*(2), 350P-351P.

Berry, R. J., Li, Z., Erickson, J. D., Li, S., Moore, C. A., Wang, H., Mulinare, J., Zhao, P., Wong, L. Y., Gindler, J., Hong, S. X., & Correa, A. (1999). Prevention of neural-tube defects with folic acid in China. China-U.S. Collaborative Project for Neural Tube Defect Prevention. *The New England Journal of Medicine*, *341*(20), 1485–1490. https://doi.org/10.1056/NEJM199911113412001

Betts, J. G., Young, K. A., Wise, J. A., Johnson, E., Poe, B., Kruse, D. H., Korol, O., Johnson, J. E., Womble, M., & DeSaix, P. (2022). Embryonic Development. In *Anatomy and Physiology* (2nd ed.). OpenStax. https://openstax.org/details/books/anatomy-and-physiology-2e

Blom, H. J., Shaw, G. M., den Heijer, M., & Finnell, R. H. (2006). Neural tube defects and folate: Case far from closed. *Nature Reviews. Neuroscience*, *7*(9), 724–731. https://doi.org/10.1038/nrn1986

Borodinsky, L. N. (2017). Xenopus laevis as a Model Organism for the Study of Spinal Cord Formation, Development, Function and Regeneration. *Frontiers in Neural Circuits*, *11*, 90. https://doi.org/10.3389/fncir.2017.00090

Bovolenta, P., & Mason, C. (1987). Growth cone morphology varies with position in the developing mouse visual pathway from retina to first targets. *The Journal of Neuroscience: The Official Journal of the Society for Neuroscience*, *7*(5), 1447–1460. https://doi.org/10.1523/JNEUROSCI.07-05-01447.1987

Brenner, S. L., & Korn, E. D. (1979). Substoichiometric concentrations of cytochalasin D inhibit actin polymerization. Additional evidence for an F-actin treadmill. *The Journal of Biological Chemistry*, *254*(20), 9982–9985.

Bridgman, P. C., & Dailey, M. E. (1989). The organization of myosin and actin in rapid frozen nerve growth cones. *The Journal of Cell Biology*, *108*(1), 95–109. https://doi.org/10.1083/jcb.108.1.95

Brown, A., Li, Y., Slaughter, T., & Black, M. M. (1993). Composite microtubules of the axon: Quantitative analysis of tyrosinated and acetylated tubulin along individual axonal microtubules. *Journal of Cell Science*, *104 (Pt 2)*, 339–352. https://doi.org/10.1242/jcs.104.2.339

Brusés, J. L., Chauvet, N., & Rutishauser, U. (2001). Membrane Lipid Rafts Are Necessary for the Maintenance of the α7 Nicotinic Acetylcholine Receptor in Somatic Spines of Ciliary Neurons. *The Journal of Neuroscience*, *21*(2), 504–512. https://doi.org/10.1523/JNEUROSCI.21-02-00504.2001

Bubb, M. R., Senderowicz, A. M., Sausville, E. A., Duncan, K. L., & Korn, E. D. (1994). Jasplakinolide, a cytotoxic natural product, induces actin polymerization and competitively inhibits the binding of phalloidin to F-actin. *Journal of Biological Chemistry*, *269*(21), 14869–14871. https://doi.org/10.1016/S0021-9258(17)36545-6

Cambray-Deakin, M. A., & Burgoyne, R. D. (1987). Acetylation and detyrosinated a-tubulins are co-localized in stable microtubules in rat meningeal fibroblasts. *Cell Motility and the Cytoskeleton*, *8*, 284–291.

Carriles, A. A., Mills, A., Munoz-Alonso, M.-J., Gutierrez, D., Dominguez, J. M., Hermoso, J. A., & Gago, F. (2021). Structural cues for understanding eEF1A2 moonlighting. *Chem Bio Chem*, *22*(2), 374–391. https://doi.org/10.1002/cbic.202000516

Casella, J. F., Flanagan, M. D., & Lin, S. (1981). Cytochalasin D inhibits actin polymerization and induces depolymerization of actin filaments formed during platelet shape change. *Nature*, *293*(5830), 302–305. https://doi.org/10.1038/293302a0

Catala, M. (2005). Embryology of the Spine and Spinal Cord. In P. Tortori-Donati & A. Rossi, *Pediatric Neuroradiology* (pp. 1533–1549). Springer Berlin Heidelberg. https://doi.org/10.1007/3-540-26398-5_38

Centers for Disease Control and Prevention (CDC). (1992). Recommendations for the use of folic acid to reduce the number of cases of spina bifida and other neural tube defects. *MMWR. Recommendations and Reports: Morbidity and Mortality Weekly Report. Recommendations and Reports*, *41*(RR-14), 1–7.

Chambers, D. M., Peters, J., & Abbott, C. M. (1998). The lethal mutation of the mouse wasted (wst) is a deletion that abolishes expression of a tissue-specific isoform of translation elongation factor 1alpha, encoded by the Eef1a2 gene. *Proc. Natl. Acad. Sci.*, *95*(8), 4463–4468.

Chang, R., & Wang, E. (2007). Mouse translation elongation factor eEF1A-2 interacts with Prdx-I to protect cells against apoptotic death induced by oxidative stress. *Journal of Cellular Biochemistry*, *100*(2), 267–278. https://doi.org/10.1002/jcb.20969

Choi, S.-W., & Mason, J. B. (2002). Folate Status: Effects on Pathways of Colorectal Carcinogenesis. *The Journal of Nutrition*, *132*(8), 2413S-2418S. https://doi.org/10.1093/jn/132.8.2413S

Connolly, J. L., Seeley, P. J., & Greene, L. A. (1985). Regulation of growth cone morphology by nerve growth factor: A comparative study by scanning electron microscopy. *Journal of Neuroscience Research*, *13*(1–2), 183–198. https://doi.org/10.1002/jnr.490130113

Cooper, G. M. (2000). Intermediate Filaments. In *The cell: A molecular approach* (2nd ed.). Sinauer Associates. https://www.ncbi.nlm.nih.gov/books/NBK9834/

Daniels, M. P. (1972). Colchicine inhibition of nerve fiber formation in vitro. *The Journal of Cell Biology*, *53*(1), 164–176. https://doi.org/10.1083/jcb.53.1.164

Datar, A., Ameeramja, J., Bhat, A., Srivastava, R., Mishra, A., Bernal, R., Prost, J., Callan-Jones, A., & Pullarkat, P. A. (2019). The Roles of Microtubules and Membrane Tension in Axonal Beading, Retraction, and Atrophy. *Biophysical Journal*, *117*(5), 880–891. https://doi.org/10.1016/j.bpj.2019.07.046

Davidson, L. A., & Keller, R. E. (1999). Neural tube closure in Xenopus laevis involves medial migration, directed protrusive activity, cell intercalation and convergent extension. *Development (Cambridge, England)*, *126*(20), 4547–4556. https://doi.org/10.1242/dev.126.20.4547

Davies, F. C. J., Hope, J. E., McLachlan, F., Marshall, G. F., Kaminioti-Dumont, L., Qarkaxhija, V., Nunez, F., Dando, O., Smith, C., Wood, E., MacDonald, J., Hardt, O., & Abbott, C. M. (2020). Recapitulation of the EEF1A2 D252H neurodevelopmental disorder-causing missense mutation in mice reveals a toxic gain of function. *Human Molecular Genetics*, *29*(10), 1592–1606. https://doi.org/10.1093/hmg/ddaa042

Davy, A., Gale, N. W., Murray, E. W., Klinghoffer, R. A., Soriano, P., Feuerstein, C., & Robbins, S. M. (1999). Compartmentalized signaling by GPI-anchored ephrin-A5 requires the Fyn tyrosine kinase to regulate cellular adhesion. *Genes & Development*, *13*(23), 3125–3135. https://doi.org/10.1101/gad.13.23.3125

De Rinaldis, M., Giorda, R., & Trabacca, A. (2020). Mild epileptic phenotype associates with de novo eef1a2 mutation: Case report and review. *Brain & Development*, *42*(1), 77–82. https://doi.org/10.1016/j.braindev.2019.08.001

Dent, E. W., & Gertler, F. B. (2003). Cytoskeletal Dynamics and Transport in Growth Cone Motility and Axon Guidance. *Neuron*, *40*(2), 209–227. https://doi.org/10.1016/S0896-6273(03)00633-0

Dent, E. W., Gupton, S. L., & Gertler, F. B. (2011). The Growth Cone Cytoskeleton in Axon Outgrowth and Guidance. *Cold Spring Harbor Perspectives in Biology*, *3*(3), a001800. https://doi.org/10.1101/cshperspect.a001800

D'Este, E., Kamin, D., Göttfert, F., El-Hady, A., & Hell, S. W. (2015). STED Nanoscopy Reveals the Ubiquity of Subcortical Cytoskeleton Periodicity in Living Neurons. *Cell Reports*, *10*(8), 1246–1251. https://doi.org/10.1016/j.celrep.2015.02.007

Djé, M. K., Mazabraud, A., Viel, A., le Maire, M., Denis, H., Crawford, E., & Brown, D. D. (1990). Three genes under different developmental control encode elongation factor 1-alpha in Xenopus laevis. *Nucleic Acids Research*, *18*(12), 3489–3493. https://doi.org/10.1093/nar/18.12.3489

Eitenmiller, R. R., Landen Jr., W. O., & Ye, L. (2007). Chapter Ten: Folate and folic acid. In *Vitamin Analysis for the Health and Food Sciences* (2 nd, pp. 443–447). CRC Press.

Elwood, P. C. (1989). Molecular cloning and characterization of the human folate-binding protein cDNA from placenta and malignant tissue culture (KB) cells. *The Journal of Biological Chemistry*, *264*(25), 14893–14901.

Encinas, M., Tansey, M. G., Tsui-Pierchala, B. A., Comella, J. X., Milbrandt, J., & Johnson, E. M. (2001). C-Src is required for glial cell line-derived neurotrophic factor (GDNF) family ligand-mediated

neuronal survival via a phosphatidylinositol-3 kinase (PI-3K)-dependent pathway. *The Journal of Neuroscience: The Official Journal of the Society for Neuroscience*, *21*(5), 1464–1472. https://doi.org/10.1523/JNEUROSCI.21-05-01464.2001

Erdogan, B., Bearce, E. A., & Lowery, L. A. (2021). Live Imaging of Cytoskeletal Dynamics in Embryonic Xenopus laevis Growth Cones and Neural Crest Cells. *Cold Spring Harbor Protocols*, *2021*(4), pdb.prot104463. https://doi.org/10.1101/pdb.prot104463

Falnikar, A., & Baas, P. W. (2009). Critical Roles for Microtubules in Axonal Development and Disease. In E. Koenig (Ed.), *Cell Biology of the Axon* (Vol. 48, pp. 47–64). Springer Berlin Heidelberg. https://doi.org/10.1007/400_2009_2

Fan, J., Mansfield, S. G., Redmond, T., Gordon-Weeks, P. R., & Raper, J. A. (1993). The organization of F-actin and microtubules in growth cones exposed to a brain-derived collapsing factor. *The Journal of Cell Biology*, *121*(3), 867–878.

Ferreira, T. A., Blackman, A. V., Oyrer, J., Jayabal, S., Chung, A. J., Watt, A. J., Sjöström, P. J., & Van Meyel, D. J. (2014). Neuronal morphometry directly from bitmap images. *Nature Methods*, *11*(10), 982–984. https://doi.org/10.1038/nmeth.3125

Friedrichson, T., & Kurzchalia, T. V. (1998). Microdomains of GPI-anchored proteins in living cells revealed by crosslinking. *Nature*, *394*(6695), 802–805. https://doi.org/10.1038/29570

Fuchs, E., & Cleveland, D. W. (1998). A structural scaffolding of intermediate filaments in health and disease. *Science (New York, N.Y.)*, *279*(5350), 514–519. https://doi.org/10.1126/science.279.5350.514

Fuchs, E., & Weber, K. (1994). INTERMEDIATE FILAMENTS: Structure, Dynamics, Function and Disease. *Annual Review of Biochemistry*, *63*(1), 345–382. https://doi.org/10.1146/annurev.bi.63.070194.002021

Gadadhar, S., Bodakuntla, S., Natarajan, K., & Janke, C. (2017). The tubulin code at a glance. *Journal of Cell Science*, *130*(8), 1347–1353. https://doi.org/10.1242/jcs.199471

Gallo, G., Yee, H. F., & Letourneau, P. C. (2002). Actin turnover is required to prevent axon retraction driven by endogenous actomyosin contractility. *The Journal of Cell Biology*, *158*(7), 1219–1228. https://doi.org/10.1083/jcb.200204140

Goddette, D. W., & Frieden, C. (1986). Actin polymerization. The mechanism of action of cytochalasin D. *Journal of Biological Chemistry*, *261*(34), 15974–15980. https://doi.org/10.1016/S0021-9258(18)66662-1

Gomez, T. M., & Letourneau, P. C. (2014). Actin dynamics in growth cone motility and navigation. *Journal of Neurochemistry*, *129*(2), 221–234. https://doi.org/10.1111/jnc.12506

Gomez, T. M., Robles, E., Poo, M., & Spitzer, N. C. (2001). Filopodial calcium transients promote substrate-dependent growth cone turning. *Science*, *291*(5510), 1983–1987. https://doi.org/10.1126/science.1056490

Gomez, T. M., & Spitzer, N. C. (1999). In vivo regulation of axon extension and pathfinding by growth-cone calcium transients. *Nature*, *397*(6717), 350–355. https://doi.org/10.1038/16927

Grapp, M., Just, I. A., Linnankivi, T., Wolf, P., Lücke, T., Häusler, M., Gärtner, J., & Steinfeld, R. (2012). Molecular characterization of folate receptor 1 mutations delineates cerebral folate transport deficiency. *Brain*, *135*(7), 2022–2031. https://doi.org/10.1093/brain/aws122

Gross, S. R., & Kinzy, T. G. (2005). Translation elongation factor 1A is essential for regulation of the actin cytoskeleton and cell morphology. *Nature Structural & Molecular Biology*, *12*(9), 772–778. https://doi.org/10.1038/nsmb979

Harma, A., Sahin, M. S., & Zorludemir, S. (2015). Effects of intraperitoneally administered folic acid on the healing of repaired tibial nerves in rats. *Journal of Reconstructive Microsurgery*, *31*(3), 191–197. https://doi.org/10.1055/s-0034-1395414

Hill, R. G., & Miller, A. A. (1974). Antagonism by folic acid of presynaptic inhibition in the rat cuneate nucleus. *British Journal of Pharmacology*, *50*(3), 425–427. https://doi.org/10.1111/j.1476-5381.1974.tb09619.x

Hisanaga, S., & Hirokawa, N. (1990). Dephosphorylation-induced interactions of neurofilaments with microtubules. *The Journal of Biological Chemistry*, *265*(35), 21852–21858.

Holm, J., Hansen, S. I., Høier-Madsen, M., & Bostad, L. (1991). High-affinity folate binding in human choroid plexus. Characterization of radioligand binding, immunoreactivity, molecular heterogeneity and hydrophobic domain of the binding protein. *Biochemical Journal*, *280*(1), 267–271. https://doi.org/10.1042/bj2800267

Huxley, J., & De Beer, G. (1934). Early amphibian development: A descriptive sketch. In *The Elements of Experimental Embryology* (pp. 13–34). Cambridge University Press.

Iskandar, B. J., Nelson, A., Resnick, D., Skene, J. H. P., Gao, P., Johnson, C., Cook, T. D., & Hariharan, N. (2004). Folic acid supplementation enhances repair of the adult central nervous system. *Annals of Neurology*, *56*(2), 221–227. https://doi.org/10.1002/ana.20174

Iskandar, B. J., Rizk, E., Meier, B., Hariharan, N., Bottiglieri, T., Finnell, R. H., Jarrard, D. F., Banerjee, R. V., Skene, J. H. P., Nelson, A., Patel, N., Gherasim, C., Simon, K., Cook, T. D., & Hogan, K. J. (2010). Folate regulation of axonal regeneration in the rodent central nervous system through DNA methylation. *The Journal of Clinical Investigation*, *120*(5), 1603–1616. https://doi.org/10.1172/JCI40000

Janmey, P. A., & Stossel, T. P. (1987). Modulation of gelsolin function by phosphatidylinositol 4,5-bisphosphate. *Nature*, *325*(6102), 362–364. https://doi.org/10.1038/325362a0

Janssen, G. M., Van Damme, H. T., Kriek, J., Amons, R., & Möller, W. (1994). The subunit structure of elongation factor 1 from Artemia. Why two alpha-chains in this complex? *Journal of Biological Chemistry*, *269*(50), 31410–31417. https://doi.org/10.1016/S0021-9258(18)31709-5

Jeganathan, S., Morrow, A., Amiri, A., & Lee, J. M. (2008). Eukaryotic elongation factor 1A2 cooperates with phosphatidylinositol-4 kinase III beta to stimulate production of filopodia through increased phosphatidylinositol-4,5 biphosphate generation. *Molecular and Cellular Biology*, *28*(14), 4549–4561. https://doi.org/10.1128/MCB.00150-08

Joshi, H. C., & Cleveland, D. W. (1989). Differential utilization of beta-tubulin isotypes in differentiating neurites. *The Journal of Cell Biology*, *109*(2), 663–673. https://doi.org/10.1083/jcb.109.2.663

Kalil, K. (1996). Chapter 3 Growth cone behaviors during axon guidance in the developing cerebral cortex. In *Progress in Brain Research* (Vol. 108, pp. 31–40). Elsevier. https://doi.org/10.1016/S0079-6123(08)62530-3

Kang, W.-B., Chen, Y.-J., Lu, D.-Y., & Yan, J.-Z. (2019). Folic acid contributes to peripheral nerve injury repair by promoting Schwann cell proliferation, migration, and secretion of nerve growth factor. *Neural Regeneration Research*, *14*(1), 132–139. https://doi.org/10.4103/1673-5374.243718

Kasahara, K., Watanabe, K., Takeuchi, K., Kaneko, H., Oohira, A., Yamamoto, T., & Sanai, Y. (2000). Involvement of gangliosides in glycosylphosphatidylinositol-anchored neuronal cell adhesion molecule TAG-1 signaling in lipid rafts. *The Journal of Biological Chemistry*, *275*(44), 34701–34709. https://doi.org/10.1074/jbc.M003163200

Koenig, E. (Ed.). (2009). *Cell Biology of the Axon* (Vol. 48). Springer Berlin Heidelberg. https://doi.org/10.1007/978-3-642-03019-2

Krieg, P. A., Varnum, S. M., Wormington, W. M., & Melton, D. A. (1989). The mRNA encoding elongation factor 1-alpha (EF-1 alpha) is a major transcript at the midblastula transition in Xenopus. *Developmental Biology*, *133*(1), 93–100. https://doi.org/10.1016/0012-1606(89)90300-x

Lallier, T. E., & DeSimone, D. W. (2000). Separation of Neural Induction and Neurulation in Xenopus. *Developmental Biology*, *225*(1), 135–150. https://doi.org/10.1006/dbio.2000.9833

Lam, D. C. L., Girard, L., Suen, W.-S., Chung, L., Tin, V. P. C., Lam, W., Minna, J. D., & Wong, M. P. (2006). Establishment and expression profiling of new lung cancer cell lines from Chinese smokers and lifetime never-smokers. *Journal of Thoracic Oncology: Official Publication of the International Association for the Study of Lung Cancer*, *1*(9), 932–942.

Lam, W. W. K., Millichap, J. J., Soares, D. C., Chin, R., McLellan, A., FitzPatrick, D. R., Elmslie, F., Lees, M. M., Schaefer, G. B., DDD study, & Abbott, C. M. (2016). Novel de novo EEF1A2 missense mutations causing epilepsy and intellectual disability. *Molecular Genetics & Genomic Medicine*, *4*(4), 465–474. https://doi.org/10.1002/mgg3.219

Lee, M. K., & Cleveland, D. W. (1996). Neuronal intermediate filaments. *Annual Review of Neuroscience*, *19*, 187–217. https://doi.org/10.1146/annurev.ne.19.030196.001155

Lee, S., Francoeur, A.-M., Liu, S., & Wang, E. (1992). Tissue-specific expression in mammalian brain, heart, and muscle of S1, a member of the elongation factor-1 alpha gene family. *The Journal of Biological Chemistry*, *267*(33), 24064–24068.

Lee, S., LeBlanc, A., Duttaroy, A., & Wang, E. (1995). Terminal differentiation-dependent alteration in the expression of translation elongation factor-1 alpha and its sister gene, S1, in neurons. *Experimental Cell Research*, *219*(2), 589–597. https://doi.org/10.1006/excr.1995.1268

Lee, S., Wolfraim, L. A., & Wang, E. (1993). Differential expression of S1 and elongation factor-1 alpha during rat development. *The Journal of Biological Chemistry*, *268*(32), 24453–24459.

Leterrier, C., Potier, J., Caillol, G., Debarnot, C., Rueda Boroni, F., & Dargent, B. (2015). Nanoscale Architecture of the Axon Initial Segment Reveals an Organized and Robust Scaffold. *Cell Reports*, *13*(12), 2781–2793. https://doi.org/10.1016/j.celrep.2015.11.051

Letourneau, P. C. (1979). Cell-substratum adhesion of neurite growth cones, and its role in neurite elongation. *Experimental Cell Research*, *124*(1), 127–138. https://doi.org/10.1016/0014-4827(79)90263-5

Letourneau, P. C. (2009). Actin in Axons: Stable Scaffolds and Dynamic Filaments. In E. Koenig (Ed.), *Cell Biology of the Axon* (Vol. 48, pp. 265–290). Springer Berlin Heidelberg. https://doi.org/10.1007/400_2009_15

Lewis, C. J., Crane, N. T., Wilson, D. B., & Yetley, E. A. (1999). Estimated folate intakes: Data updated to reflect food fortification, increased bioavailability, and dietary supplement use. *The American Journal of Clinical Nutrition*, *70*(2), 198–207. https://doi.org/10.1093/ajcn.70.2.198

Li, L., & Yang, X.-J. (2015). Tubulin acetylation: Responsible enzymes, biological functions and human diseases. *Cellular and Molecular Life Sciences*, *72*(22), 4237–4255. https://doi.org/10.1007/s00018-015-2000-5

Liem, R. K. H., & Messing, A. (2009). Dysfunctions of neuronal and glial intermediate filaments in disease. *The Journal of Clinical Investigation*, *119*(7), 1814–1824. https://doi.org/10.1172/JCI38003

Liu, G., Grant, W. M., Persky, D., Latham, V. M., Singer, R. H., & Condeelis, J. (2002). Interactions of elongation factor 1alpha with F-actin and beta-actin mRNA: Implications for anchoring mRNA in cell protrusions. *Molecular Biology of the Cell*, *13*(2), 579–592. https://doi.org/10.1091/mbc.01-03-0140

Lowery, L. A., Faris, A. E. R., Stout, A., & Van Vactor, D. (2012). Neural Explant Cultures from Xenopus laevis. *Journal of Visualized Experiments: JoVE*, *68*, e4232. https://doi.org/10.3791/4232

Lowery, L. A., Stout, A., Faris, A. E., Ding, L., Baird, M. A., Davidson, M. W., Danuser, G., & Van Vactor, D. (2013). Growth cone-specific functions of XMAP215 in restricting microtubule dynamics and promoting axonal outgrowth. *Neural Development*, *8*, 22. https://doi.org/10.1186/1749-8104-8-22

Lowery, L. A., & Vactor, D. V. (2009). The trip of the tip: Understanding the growth cone machinery. *Nature Reviews Molecular Cell Biology*, *10*(5), 332–343. https://doi.org/10.1038/nrm2679

Lucaj, C. M., Evans, M. F., Nwagbara, B. U., Ebbert, P. T., Baker, C. C., Volk, J. G., Francl, A. F., Ruvolo, S. P., & Lowery, L. A. (2015). Xenopus TACC1 is a microtubule plus-end tracking protein that can regulate microtubule dynamics during embryonic development. *Cytoskeleton (Hoboken)*, *72*(5), 225–234. https://doi.org/10.1002/cm.21224

Luhrs, C. A., & Slomiany, B. L. (1989). A human membrane-associated folate binding protein is anchored by a glycosyl-phosphatidylinositol tail. *The Journal of Biological Chemistry*, *264*(36), 21446–21449.

Martens, J. R., Navarro-Polanco, R., Coppock, E. A., Nishiyama, A., Parshley, L., Grobaski, T. D., & Tamkun, M. M. (2000). Differential Targeting of Shaker-like Potassium Channels to Lipid Rafts. *Journal of Biological Chemistry*, *275*(11), 7443–7446. https://doi.org/10.1074/jbc.275.11.7443

Martin, J. B., Muccioli, M., Herman, K., Finnell, R. H., & Plageman, T. F. (2019). Folic acid modifies the shape of epithelial cells during morphogenesis via a Folr1 and MLCK dependent mechanism. *Biology Open*, *8*(1), bio041160. https://doi.org/10.1242/bio.041160

Marx, A., Godinez, W. J., Tsimashchuk, V., Bankhead, P., Rohr, K., & Engel, U. (2013). Xenopus cytoplasmic linker-associated protein 1 (XCLASP1) promotes axon elongation and advance of pioneer microtubules. *Molecular Biology of the Cell*, *24*(10), 1544–1558. https://doi.org/10.1091/mbc.E12-08-0573

Matherly, L. H., & Goldman, I. D. (2003). Membrane Transport of Folate. In *Vitamins and Hormones* (Vol. 66, pp. 403–456). Elsevier Science (USA).

Matsue, H., Rothberg, K. G., Takashima, A., Kamen, B. A., Anderson, R. G., & Lacey, S. W. (1992). Folate receptor allows cells to grow in low concentrations of 5-methyltetrahydrofolate. *Proceedings of the National Academy of Sciences of the United States of America*, *89*(13), 6006–6009. https://doi.org/10.1073/pnas.89.13.6006

Mattson, M. P., & Shea, T. B. (2003). Folate and homocysteine metabolism in neural plasticity and neurodegenerative disorders. *Trends in Neurosciences*, *26*(3), 137–146. https://doi.org/10.1016/S0166-2236(03)00032-8

Matus, A. (1990). Microtubule-associated proteins and the determination of neuronal form. *Journal De Physiologie*, *84*(1), 134–137.

McFarlane, S., & Lom, B. (2012). The *Xenopus* retinal ganglion cell as a model neuron to study the establishment of neuronal connectivity. *Developmental Neurobiology*, *72*(4), 520–536. https://doi.org/10.1002/dneu.20928

Meijering, E., Dzyubachyk, O., & Smal, I. (2012). Methods for cell and particle tracking. *Methods in Enzymology*, *504*, 183–200. https://doi.org/10.1016/B978-0-12-391857-4.00009-4

Mendoza, M. B., Gutierrez, S., Ortiz, R., Moreno, D. F., Dermit, M., Dodel, M., Rebollo, E., Bosch, M., Mardakheh, F. K., & Gallego, C. (2021). The elongation factor eEF1A2 controls translation and actin dynamics in dendritic spines. *Science Signaling*, *14*(691), eabf5594. https://doi.org/10.1126/scisignal.abf5594

Miranda-Morales, E., Meier, K., Sandoval-Carrillo, A., Salas-Pacheco, J., Vázquez-Cárdenas, P., & Arias-Carrión, O. (2017). Implications of DNA Methylation in Parkinson's Disease. *Frontiers in Molecular Neuroscience*, *10*, 225. https://doi.org/10.3389/fnmol.2017.00225

MRC Vitamin Study Research Group. (1991). Prevention of neural tube defects: Results of the Medical Research Council Vitamin Study. MRC Vitamin Study Research Group. *Lancet (London, England)*, *338*(8760), 131–137.

Munshi, R., Kandl, K. A., Carr-Schmid, A., Whitacre, J. L., Adams, A. E., & Kinzy, T. G. (2001). Overexpression of translation elongation factor 1A affects the organization and function of the actin cytoskeleton in yeast. *Genetics*, *157*(4), 1425–1436. https://doi.org/10.1093/genetics/157.4.1425

Murray, J. W., Edmonds, B. T., Liu, G., & Condeelis, J. (1996). Bundling of Actin Filaments by Elongation Factor 1 alpha Inhibits Polymerization at Filament Ends. *The Journal of Cell Biology*, *135*(5), 1309–1321.

Nakajima, J., Okamoto, N., Tohyama, J., Kato, M., Arai, H., Funahashi, O., Tsurusaki, Y., Nakashima, M., Kawashima, H., Saitsu, H., Matsumoto, N., & Miyake, N. (2015). De novo EEF1A2 mutations in patients with characteristic facial features, intellectual disability, autistic behaviors and epilepsy. *Clinical Genetics*, *87*(4), 356–361. https://doi.org/10.1111/cge.12394

Negrutskii, B. S., & El'skaya, A. V. (1998). Eukaryotic translation elongation factor 1 alpha: Structure, expression, functions, and possible role in aminoacyl-tRNA channeling. *Progress in Nucleic Acid Research and Molecular Biology*, *60*, 47–78.

Nieuwkoop, P. D., & Faber, J. (Eds.). (1994). *Normal table of Xenopus laevis (Daudin): A systematical and chronological survey of the development from the fertilized egg till the end of metamorphosis*. Garland Pub.

Nishida, E. (1985). Opposite effects of cofilin and profilin from porcine brain on rate of exchange of actin-bound adenosine 5'-triphosphate. *Biochemistry*, *24*(5), 1160–1164. https://doi.org/10.1021/bi00326a015

Nordlander, R. H. (1987). Axonal growth cones in the developing amphibian spinal cord. *The Journal of Comparative Neurology*, *263*(4), 485–496. https://doi.org/10.1002/cne.902630403

Nsamba, E. T., & Gupta, M. L. (2022). Tubulin isotypes – functional insights from model organisms. *Journal of Cell Science*, *135*(9), jcs259539. https://doi.org/10.1242/jcs.259539

Pacheco, A., & Gallo, G. (2016). Actin filament-microtubule interactions in axon initiation and branching. *Brain Research Bulletin*, *126*, 300–310. https://doi.org/10.1016/j.brainresbull.2016.07.013

Pavlov, D., Muhlrad, A., Cooper, J., Wear, M., & Reisler, E. (2007). Actin filament severing by cofilin. *Journal of Molecular Biology*, *365*(5), 1350–1358. https://doi.org/10.1016/j.jmb.2006.10.102

Piedrahita, J. A., Oetama, B., Bennett, G. D., Van Waes, J., Kamen, B. A., Richardson, J., Lacey, S. W., Anderson, R. G. W., & Finnell, R. H. (1999). Mice lacking the folic acid-binding protein Folbp1 are defective in early embryonic development. *Nature Genetics*, *23*(2), 228–232. https://doi.org/10.1038/13861

Pollard, T. D. (2016). Actin and Actin-Binding Proteins. *Cold Spring Harbor Perspectives in Biology*, *8*(8), a018226. https://doi.org/10.1101/cshperspect.a018226

Prasad, P. D., Ramamoorthy, S., Moe, A. J., Smith, C. H., Leibach, F. H., & Ganapathy, V. (1994). Selective expression of the high-affinity isoform of the folate receptor (FR-α) in the human placental syncytiotrophoblast and choriocarcinoma cells. *Biochimica et Biophysica Acta (BBA) - Molecular Cell Research*, *1223*(1), 71–75. https://doi.org/10.1016/0167-4889(94)90074-4

Prochniewicz, E., Janson, N., Thomas, D. D., & De la Cruz, E. M. (2005). Cofilin increases the torsional flexibility and dynamics of actin filaments. *Journal of Molecular Biology*, *353*(5), 990–1000. https://doi.org/10.1016/j.jmb.2005.09.021

Qiu, A., Jansen, M., Sakaris, A., Min, S. H., Chattopadhyay, S., Tsai, E., Sandoval, C., Zhao, R., Akabas, M. H., & Goldman, I. D. (2006). Identification of an intestinal folate transporter and the molecular basis for hereditary folate malabsorption. *Cell*, *127*(5), 917–928. https://doi.org/10.1016/j.cell.2006.09.041

Qiu, A., Min, S. H., Jansen, M., Malhotra, U., Tsai, E., Cabelof, D. C., Matherly, L. H., Zhao, R., Akabas, M. H., & Goldman, I. D. (2007). Rodent intestinal folate transporters (SLC46A1): Secondary structure, functional properties, and response to dietary folate restriction. *American Journal of Physiology. Cell Physiology*, *293*(5), C1669-1678. https://doi.org/10.1152/ajpcell.00202.2007

Qiu, F.-N., Huang, Y., Chen, D.-Y., Li, F., Wu, Y.-A., Wu, W.-B., & Huang, X.-L. (2016). Eukaryotic elongation factor-1α 2 knockdown inhibits hepatocarcinogenesis by suppressing PI3K/Akt/NF-κB signaling. *World Journal of Gastroenterology*, *22*(16), 4226–4237. https://doi.org/10.3748/wjg.v22.i16.4226

Rao, M. V., Mohan, P. S., Kumar, A., Yuan, A., Montagna, L., Campbell, J., Veeranna, Espreafico, E. M., Julien, J. P., & Nixon, R. A. (2011). The myosin Va head domain binds to the neurofilament-L rod and modulates endoplasmic reticulum (ER) content and distribution within axons. *PloS One*, *6*(2), e17087. https://doi.org/10.1371/journal.pone.0017087

Roberts, A., & Clarke, J. D. (1982). The neuroanatomy of an amphibian embryo spinal cord. *Philosophical Transactions of the Royal Society of London. Series B, Biological Sciences*, *296*(1081), 195–212. https://doi.org/10.1098/rstb.1982.0002

Ross, J. F., Chaudhuri, P. K., & Ratnam, M. (1994). Differential regulation of folate receptor isoforms in normal and malignant tissues in vivo and in established cell lines. *Cancer*, *73*(9), 2239–2456.

Ruchhoeft, M. L., Ohnuma, S., McNeill, L., Holt, C. E., & Harris, W. A. (1999). The neuronal architecture of Xenopus retinal ganglion cells is sculpted by rho-family GTPases in vivo. *The Journal of Neuroscience: The Official Journal of the Society for Neuroscience*, *19*(19), 8454–8463. https://doi.org/10.1523/JNEUROSCI.19-19-08454.1999

Ruest, L.-B., Marcotte, R., & Wang, E. (2002). Peptide elongation factor eEF1A-2/S1 expression in cultured differentiated myotubes and its protective effect against caspase-3-mediated apoptosis. *The Journal of Biological Chemistry*, *277*(7), 5418–5425. https://doi.org/10.1074/jbc.M110685200

Sabharanjak, S., & Mayor, S. (2004). Folate receptor endocytosis and trafficking. *Advanced Drug Delivery Reviews*, *56*(8), 1099–1109. https://doi.org/10.1016/j.addr.2004.01.010

Saitsu, H., Ishibashi, M., Nakano, H., & Shiota, K. (2003). Spatial and temporal expression of *folate-binding protein 1* (*Fbp1*) is closely associated with anterior neural tube closure in mice. *Developmental Dynamics*, *226*(1), 112–117. https://doi.org/10.1002/dvdy.10203

Santos, R. A., Rio, R. D., & Cohen-Cory, S. (2020). Imaging the Dynamic Branching and Synaptic Differentiation of Xenopus Optic Axons In Vivo. *Cold Spring Harbor Protocols*, *2020*(11). https://doi.org/10.1101/pdb.prot106823

Sanyal, C., Pietsch, N., Ramirez Rios, S., Peris, L., Carrier, L., & Moutin, M.-J. (2023). The detyrosination/re-tyrosination cycle of tubulin and its role and dysfunction in neurons and cardiomyocytes. *Seminars in Cell & Developmental Biology*, *137*, 46–62. https://doi.org/10.1016/j.semcdb.2021.12.006

Schindelin, J., Arganda-Carreras, I., Frise, E., Kaynig, V., Longair, M., Pietzsch, T., Preibisch, S., Rueden, C., Saalfeld, S., Schmid, B., Tinevez, J.-Y., White, D. J., Hartenstein, V., Eliceiri, K., Tomancak, P., & Cardona, A. (2012). Fiji: An open-source platform for biological-image analysis. *Nature Methods*, *9*(7), 676–682. https://doi.org/10.1038/nmeth.2019

Schliwa, M. (1982). Action of cytochalasin D on cytoskeletal networks. *The Journal of Cell Biology*, *92*(1), 79–91. https://doi.org/10.1083/jcb.92.1.79

Schron, C. M., Washington, C., & Blitzer, B. L. (1985). The transmembrane pH gradient drives uphill folate transport in rabbit jejunum. Direct evidence for folate/hydroxyl exchange in brush border membrane vesicles. *The Journal of Clinical Investigation*, *76*(5), 2030–2033. https://doi.org/10.1172/JCI112205

Selhub, J., & Franklin, W. A. (1984). The folate-binding protein of rat kidney. Purification, properties, and cellular distribution. *Journal of Biological Chemistry*, *259*(10), 6601–6606. https://doi.org/10.1016/S0021-9258(20)82184-X

Shen, F., Wu, M., Ross, J. F., Miller, D., & Ratnam, M. (1995). Folate receptor type γ is primarily a secretory protein due to lack of an efficient signal for glycosylphosphatidylinositol modification: Protein characterization and cell type specificity. *Biochemistry*, *34*(16), 5660–5665.

Shiina, N., Gotoh, Y., Kubomura, N., Iwamatsu, A., & Nishida, E. (1994). Microtubule Severing by Elongation Factor 1α. *Science*, *266*(5183), 282–285. https://doi.org/10.1126/science.7939665

Shirkey, N. J., Manitt, C., Zuniga, L., & Cohen-Cory, S. (2012). Dynamic responses of Xenopus retinal ganglion cell axon growth cones to netrin-1 as they innervate their in vivo target. *Developmental Neurobiology*, *72*(4), 628–648. https://doi.org/10.1002/dneu.20967

Sholl, D. A. (1953). Dendritic organization in the neurons of the visual and motor cortices of the cat. *Journal of Anatomy*, *87*(4), 387–406.

Shultz, L. D., Sweet, H. O., Davisson, M. T., & Coman, D. R. (1982). "Wasted", a new mutant of the mouse with abnormalities characteristic of ataxia telangiectasia. *Nature*, *297*, 402–404. https://doi.org/10.1038/297402a0

Simons, K., & Ikonen, E. (1997). Functional rafts in cell membranes. *Nature*, *387*(6633), 569–572. https://doi.org/10.1038/42408

Simons, K., & Toomre, D. (2000). Lipid rafts and signal transduction. *Nature Reviews Molecular Cell Biology*, *1*(1), 31–39. https://doi.org/10.1038/35036052

Sive, H. L., Grainger, R., & Harland, R. M. (2010). *Early development of Xenopus laevis: A laboratory manual*. Cold Spring Harbor Laboratory Press.

Slater, P. G., Hayrapetian, L., & Lowery, L. A. (2017). Xenopus laevis as a model system to study cytoskeletal dynamics during axon pathfinding. *Genesis*, *55*(1–2). https://doi.org/10.1002/dvg.22994

Smithells, R. W., Sheppard, S., & Schorah, C. J. (1976). Vitamin deficiencies and neural tube defects. *Archives of Disease in Childhood*, *51*(12), 944–950. https://doi.org/10.1136/adc.51.12.944

Song, H. J., Ming, G. L., & Poo, M. M. (1997). cAMP-induced switching in turning direction of nerve growth cones. *Nature*, *388*(6639), 275–279. https://doi.org/10.1038/40864

Spector, I., Braet, F., Shochet, N. R., & Bubb, M. R. (1999). New anti-actin drugs in the study of the organization and function of the actin cytoskeleton. *Microscopy Research and Technique*, *47*, 18–37.

Spector, R. (1977). Identification of folate binding macromolecule in rabbit choroid plexus. *Journal of Biological Chemistry*, *252*(10), 3364–3370. https://doi.org/10.1016/S0021-9258(17)40398-X

Spector, R. G. (1972). Influence of folic acid on excitable tissues. *Nature: New Biology*, *240*(103), 247–249. https://doi.org/10.1038/newbio240247b0

Stover, P. J. (2004). Physiology of folate and vitamin B12 in health and disease. *Nutrition Reviews*, *62*(6 Pt 2), S3-12; discussion S13. https://doi.org/10.1111/j.1753-4887.2004.tb00070.x

Tansey, M. G., Baloh, R. H., Milbrandt, J., & Johnson, E. M. (2000). GFRalpha-mediated localization of RET to lipid rafts is required for effective downstream signaling, differentiation, and neuronal survival. *Neuron*, *25*(3), 611–623. https://doi.org/10.1016/s0896-6273(00)81064-8

Taylor, J. S., & Roberts, A. (1983). The early development of the primary sensory neurones in an amphibian embryo: A scanning electron microscope study. *Journal of Embryology and Experimental Morphology*, *75*, 49–66.

Tessier-Lavigne, M., & Goodman, C. S. (1996). The molecular biology of axon guidance. *Science*, *274*(5290), 1123–1133.

Tirnauer, J. S., Grego, S., Salmon, E., & Mitchison, T. J. (2002). EB1-Microtubule Interactions in Xenopus egg extracts: Role of EB1 in microtubule stabilization and mechanisms of targeting to microtubules. *Molecular Biology of the Cell*, *13*, 3614–3626.

Tischfield, M. A., & Engle, E. C. (2010). Distinct alpha- and beta-tubulin isotypes are required for the positioning, differentiation and survival of neurons: New support for the “multi-tubulin” hypothesis. *Bioscience Reports*, *30*(5), 319–330. https://doi.org/10.1042/BSR20100025

Tomlinson, V. A., Newbery, H. J., Wray, N. R., Jackson, J., Larionov, A., Miller, W. R., Dixon, J. M., & Abbott, C. M. (2005). Translation elongation factor eEF1A2 is a potential oncoprotein that is overexpressed in two-thirds of breast tumours. *BMC Cancer*, *5*, 113. https://doi.org/10.1186/1471-2407-5-113

Tsui-Pierchala, B. A., Encinas, M., Milbrandt, J., & Johnson, E. M. (2002). Lipid rafts in neuronal signaling and function. *Trends in Neurosciences*, *25*(8), 412–417.

Varma, R., & Mayor, S. (1998). GPI-anchored proteins are organized in submicron domains at the cell surface. *Nature*, *394*(6695), 798–801. https://doi.org/10.1038/29563

Wagner, O. I., Lifshitz, J., Janmey, P. A., Linden, M., McIntosh, T. K., & Leterrier, J.-F. (2003). Mechanisms of mitochondria-neurofilament interactions. *The Journal of Neuroscience: The Official Journal of the Society for Neuroscience*, *23*(27), 9046–9058. https://doi.org/10.1523/JNEUROSCI.23-27-09046.2003

Wallingford, J. B. (2010). Low-magnification live imaging of Xenopus embryos for cell and developmental biology. *Cold Spring Harbor Protocols*, *2010*(5), pdb.prot5425. https://doi.org/10.1101/pdb.prot5425

Wallingford, J. B., Niswander, L. A., Shaw, G. M., & Finnell, R. H. (2013). The continuing challenge of understanding, preventing, and treating neural tube defects. *Science (New York, N.Y.)*, *339*(6123), 1222002. https://doi.org/10.1126/science.1222002

Walsh, F. S., & Doherty, P. (1997). NEURAL CELL ADHESION MOLECULES OF THE IMMUNOGLOBULIN SUPERFAMILY: Role in Axon Growth and Guidance. *Annual Review of Cell and Developmental Biology*, *13*(1), 425–456. https://doi.org/10.1146/annurev.cellbio.13.1.425

Wang, Y., Zhao, R., Russell, R. G., & Goldman, I. D. (2001). Localization of the murine reduced folate carrier as assessed by immunohistochemical analysis. *Biochimica et Biophysica Acta (BBA) - Biomembranes*, *1513*(1), 49–54. https://doi.org/10.1016/S0005-2736(01)00340-6

Webster, D. R., & Borisy, G. G. (1989). Microtubules are acetylated in domains that turn over slowly. *Journal of Cell Science*, *92 (Pt 1)*, 57–65. https://doi.org/10.1242/jcs.92.1.57

Whetstine, J. R., Flatley, R. M., & Matherly, L. H. (2002). The human reduced folate carrier gene is ubiquitously and differentially expressed in normal human tissues: Identification of seven non-coding exons and characterization of a novel promoter. *Biochemical Journal*, *367*(3), 629–640. https://doi.org/10.1042/bj20020512

Woloschak, G. E., Rodriguez, M., & Krco, C. J. (1987). Characterization of immunologic and neuropathologic abnormalities in wasted mice. *Journal of Immunology*, *138*(8), 2493–2499.

Worst, T. S., Waldbillig, F., Abdelhadi, A., Weis, C.-A., Gottschalt, M., Steidler, A., von Hardenberg, J., Michel, M. S., & Erben, P. (2017). The EEF1A2 gene expression as risk predictor in localized prostate cancer. *BMC Urology*, *17*(1), 86. https://doi.org/10.1186/s12894-017-0278-3

Xu, K., Zhong, G., & Zhuang, X. (2013). Actin, Spectrin, and Associated Proteins Form a Periodic Cytoskeletal Structure in Axons. *Science*, *339*(6118), 452–456. https://doi.org/10.1126/science.1232251

Xu, X., Fu, A. K. Y., Ip, F. C. F., Wu, C., Duan, S., Poo, M., Yuan, X., & Ip, N. Y. (2005). Agrin regulates growth cone turning of Xenopus spinal motoneurons. *Development (Cambridge, England)*, *132*(19), 4309–4316. https://doi.org/10.1242/dev.02016

Yamada, K. M., Spooner, B. S., & Wessells, N. K. (1970). Axon growth: Roles of microfilaments and microtubules. *Proceedings of the National Academy of Sciences of the United States of America*, *66*(4), 1206–1212. https://doi.org/10.1073/pnas.66.4.1206

Yang, S., Lu, M., Chen, Y., Meng, D., Sun, R., Yun, D., Zhao, Z., Lu, D., & Li, Y. (2015). Overexpression of eukaryotic elongation factor 1 alpha-2 is associated with poorer prognosis in patients with gastric cancer. *Journal of Cancer Research and Clinical Oncology*, *141*(7), 1265–1275. https://doi.org/10.1007/s00432-014-1897-7

Yuan, A., Rao, M. V., Veeranna, & Nixon, R. A. (2017). Neurofilaments and Neurofilament Proteins in Health and Disease. *Cold Spring Harbor Perspectives in Biology*, *9*(4), a018309. https://doi.org/10.1101/cshperspect.a018309

Zhao, R., & Goldman, I. D. (2007). The molecular identity and characterization of a Proton-Coupled Folate Transporter—PCFT; biological ramifications and impact on the activity of pemetrexed—12 06 06. *Cancer and Metastasis Reviews*, *26*(1), 129–139. https://doi.org/10.1007/s10555-007-9047-1

Zhao, R., Matherly, L. H., & Goldman, I. D. (2009). Membrane transporters and folate homeostasis: Intestinal absorption and transport into systemic compartments and tissues. *Expert Reviews in Molecular Medicine*, *11*, e4. https://doi.org/10.1017/S1462399409000969

Zheng, J. Q., Wan, J. J., & Poo, M. M. (1996). Essential role of filopodia in chemotropic turning of nerve growth cone induced by a glutamate gradient. *The Journal of Neuroscience: The Official Journal*

of the Society for Neuroscience, *16*(3), 1140–1149. https://doi.org/10.1523/JNEUROSCI.16-03-01140.1996

Zhu, H., Lam, D. C. L., Han, K. C., Tin, V. P. C., Suen, W. S., Wang, E., Lam, W. K., Cai, W. W., Chung, L. P., & Wong, M. P. (2007). High resolution analysis of genomic aberrations by metaphase and array comparative genomic hybridization identifies candidate tumour genes in lung cancer cell lines. *Cancer Letters*, *245*(1–2), 303–314. https://doi.org/10.1016/j.canlet.2006.01.020